Antibodies that react specifically with EphA10 could have diagnostic and therapeutic utility, particularly if they show functional blocking activity. Towards this end, we previously created murine IgG reactive with EphA10 [5]. This anti-EphA10 antibody, in full IgG format, showed anti-tumor activity against breast cancer model mice, however, the effect of BsAb against EphA10-expressing cells was not clear. Here we describe the development of an anti-EphA10 and CD3 BsAb in diabody format. The bivalent nature of diabodies is advantageous for targeting and they provide a flexible platform for development of targeted therapeutics. The anti-EphA10 and CD3 diabody showed cytotoxicity *in vitro* against EphA10-expressing cells.

2. Materials and methods

2.1. Cell lines and culture

Hybridoma 38.1 (mouse Hybridoma HB-231) and MDA-MB-435 (human breast cancer cell line HTB-129) cells were obtained from American Type Culture Collection (ATCC, Rockville, MD) and cultured under the recommended conditions. Human cells that overexpressed EphA10, MDA-MB-435 (MDA-MB-435^{EphA10}), were established in our laboratory. In brief, a lentiviral vector encoding human EphA10 was transfected into MDA-MB-435 cells and stably transfected cells were obtained by Blasticidin (Invitrogen) selection. A hybridoma producing anti-EphA10 IgG was established from splenocytes of a human EphA10-immunized mouse by fusion with a mouse myeloma line.

2.2. Cloning of variable (V) immunoglobulin domains

The genes of V light-chain (VL) and V heavy-chain (VH) domains from each hybridoma were subcloned using 5′-Full RACE kits (Takara Bio, Kyoto, Japan). The amplified DNA was directionally subcloned into a plasmid vector using the TOPO TA cloning kit (Invitrogen) and sequenced using a 3130xl Genetic Analyzer (Applied Biosystems, Carlsbad, CA).

2.3. Vector construction

The vectors to express the bispecific antibody or single chain Fv (scFv), respectively, were constructed as described previously [14]. The primer sequences are shown in Table 1. To construct the co-expression vector, two additional restriction sites (*Sac*II, *Spe*I) were inserted into the pET20b vector (Invitrogen) and the new vector was named pET20b (SS+). The *E. coli* TOP10 strain (Invitrogen) was used to subclone target genes. To obtain a scFv A (EphA10-VL-Linker-CD3-VH) and a scFv B (CD3-VL-Linker-EphA10-VH), the corresponding VL and VH regions were cloned into separate vectors as templates for VL- and VH-specific PCR using the primer pairs 5′ *Nco*I-VL (hEphA10 or hCD3)/3′ VL (hEphA10 or hCD3)-Linker and 5′ Linker-VH (hEphA10 and hCD3)/3′ VH (hCD3)-*Not*I (scFv A) or 3′ VH (hEphA10)-FLAG tag (DYKDDDDKA) *Xho*I (scFv B), respectively. Overlapping complementary sequences were introduced into the PCR products, which combined to form the coding sequence of the 5-amino acid (G_4S) Linker during the subsequent fusion PCR. This amplification step was performed with the primer pair 5′ *Nco*I-VL (hEphA10 or hCD3)/3′ VH (hCD3)-*Not*I (scFv A) or 3′ VH (hEphA10)-FLAG tag *Xho*I (scFv B), and the resulting fusion product was cleaved with the restriction enzymes *Nco*I and *Not*I (scFv A) or *Xho*I (scFv B), then cloned into the pET20b (SS+) vector (scFv A) and pET20b vector (scFv B). Next, to construct the bispecific antibody (diabody) expression vector, the previously described scFv B vector was used as a template for scFv-specific PCR with the primer pair 5′ *Sac*II-pelB/3′ FLAG-tag-stop-*Spe*I. The PCR product was cleaved with the restriction enzymes *Sac*II and *Spe*I, then cloned into the pET20b (SS+) scFv A vector (pET20b (SS+) diabody).

2.4. Expression and purification of the diabody

In order to express the bispecific diabody, plasmid pET20b (SS+) diabody was transformed into *E. coli* BL21 (DE3) Star (Invitrogen). *Escherichia coli* cells containing the recombinant plasmids were inoculated into 3 ml of 2xYT medium containing 1 mg/ml ampicillin. Overnight cultures were transferred to 300 ml of fresh medium and were grown at 37 °C until they reached an A_{600} = 0.8. Isopropyl-β-D-thiogalactopyranoside (IPTG) was added to a final concentration of 0.5 mM and the cultures were further grown overnight at 20 °C. *E. coli* cells were collected by centrifugation (8000*g* for 20 min at 4 °C) and re-suspended in Osmotic Shock buffer (20 mM Tris–HCl, pH 8.0, 0.5 M sucrose, and EDTA added to 0.1 mM final). After 1 h incubation at 4 °C, the cells were shocked by adding ice water and then centrifuged (8000*g* for 30 min at 4 °C). The diabody-containing supernatant was brought to 60% ammonium sulfate and stirred gently overnight. The diabody was precipitated by centrifugation (8000*g* for 30 min at 4 °C). The protein pellet was resuspended in phosphate-buffered saline (PBS) buffer and dialysed exhaustively against PBS at 4 °C.

After dialysis, the diabody was purified by immobilized metal affinity chromatography (IMAC). The diabody was eluted using 150 mM imidazole/PBS (Db-1 Elution) and 300 mM imidazole/PBS (Db-2 Elution) buffers. Each fraction was subjected to gel filtration chromatography with a Superdex200 prep grade column (GE Healthcare, Little Chalfont Bucks, UK) equilibrated in PBS. SDS–PAGE and Western blot analysis with an anti-His or anti-FLAG tag antibody were performed to detect and confirm the size and purity of the diabody-containing fractions. Purified proteins were concentrated in PBS by ultrafiltration with a Centriprep® 30 K or 50 K

Table 1
Oligonucleotide sequences of PCR primers used for construction of diabody (EphA10/CD3) vector.

Primer	Nucleotide sequence (5′–3′)[a]
5′ NcoI-VL (hEphA10)	NNNCCATGGCCAGTTTTGTGATGACCCAGACTCCC
3′ VL (hEphA10)-Linker	CTGGCTACCACCACCACCAGCCCGTTTGATTTCCAGCTTGGT
5′ Linker-VH (hEphA10)	GAAAGGTGGTGGTGGTAGCCAGGTTCTGCTGCAGCAGTCT
3′ VH (hEphA10)-FLAG-*Xho*I	NNNCTCGAGTCATCAGGCCTTGTCATCGTCATCCTTGTAGTCTGAGGAGACGGTGACTGAGGTT
5′ *Nco*I-VL (hCD3)	NNNCCATGGCCCAAATTGTTCTCACCCAGTCTCCAG
3′ VL (hCD3)-Linker	CTGGCTACCACCACCACCTTTCAGCTCCAGCTTGGTCCC
5′ Linker-VH (hCD3))	GCTGGTGGTGGTGGTAGCCAGGTCCAGCTGCAGCAGT
3′ VH (hCD3)-*Not*I	NNNGCGGCCGCTGAGGAGACGGTGACTGAGGTT
5′ *Sac*II-pelB	NNNCCGCGGATGAAATACCTGCTGCCGACCG
3′ FLAG-tag-stop-*Spe*I	NNNACTAGTTCATCAGGCCTTGTCATCGTCATC

[a] The restriction enzyme site is underlined.

device (Millipore, Billerica, MA, USA), and protein concentrations were estimated using a Coomassie Plus Protein Assay kit (Thermo Fisher Scientific, Rockford, IL).

2.5. Flow cytometric analysis

MDA-MB-435 or MDA-MB-435^{EphA10} (5×10^5 cells) were suspended in Suspension buffer (2% FBS containing PBS) and incubated with 20 μg diabody or 2 μg control IgG (anti-EphA10, anti-CD3) for 1 h on ice, respectively. After washing with Suspension buffer, the cells were incubated with Surelight P3 (614 nm excitation and 662 nm emission) labeled antibodies against the His tag (Columbia Biosciences, Frederick, MD) and Surelight P3 labeled antibodies against the mouse IgG (Columbia Biosciences) for 1 h on ice. The cells were washed again and resuspended in 500 μL Suspension buffer and flow cytometric analysis was performed (FACScanto; BD Biosciences, San Jose, CA). All tests were carried out in triplicate.

2.6. Cytotoxicity assays

Cytotoxicity assays were performed as described previously with slight modifications [14]. In brief, MDA-MB-435^{EphA10} cells and MDA-MB-435 parent cells as target cells (10^3 cells/well) were added to 96-well plates with 10% FBS containing D-MEM at 37 °C in a humidified atmosphere containing 5% CO_2. After overnight culture, supernatants were removed and non-stimulated human PBMC from healthy donors as effector cells were added to an effector-to-target (E/T) ratio of 10 with each of the antibodies (0.1–10 μg/mL), respectively. After 48 h of incubation, lactate dehydrogenase (LDH) released into the supernatant was measured using a CytoTox 96® non-radioactive cytotoxicity assay (Promega, Madison, WI). Percentages of specific lysis were calculated according to the formula: % cytotoxicity = [(experimental release) − (effector spontaneous release) − (target spontaneous release)]/[(target maximum release) − (target spontaneous release)] × 100. All tests were carried out in triplicate.

2.7. Statistical analysis

Differences in cytotoxicity assay results between the control and target groups were compared using the unpaired Student's *t*-test.

3. Result and discussion

3.1. Formulations of diabody binding to EphA10 and CD3

A BsAb was constructed using two different scFv fragments (scFv A and scFv B) derived from the anti-EphA10 IgG and anti-CD3 IgG. His-tagged and FLAG-tagged VL-VH chain (EphA10-VL-Linker-CD3-VH; scFv A and CD3-VL-Linker- EphA10-VH; scFv

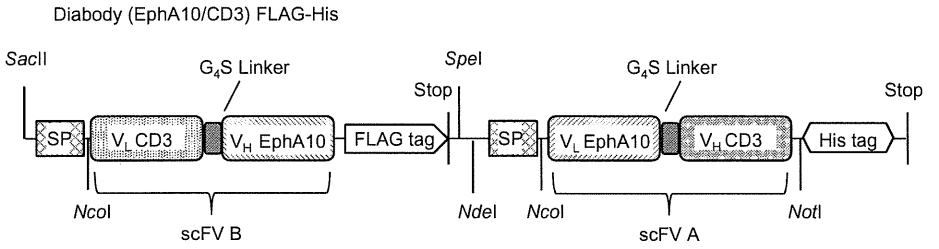

Fig. 1. Construction of the diabody-expressing vector.

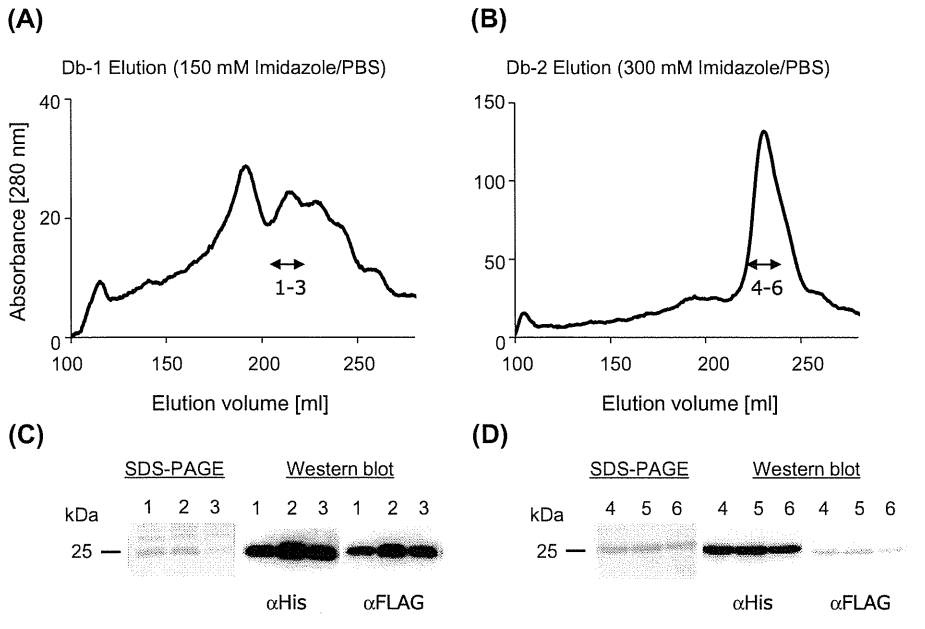

Fig. 2. Characteristics of diabody (Db-1 and Db-2). Gel filtration chromatography profile of diabodies, which were purified by IMAC. (A) 150 mM imidazole elution pattern (Db-1 as heterodimer) and (B) 300 mM imidazole elution pattern (Db-2 as homodimer). SDS–PAGE and Western blot analysis of dimeric Db-1 (C) and Db-2 (D). The line indicates the apparent molecular weight (25 kDa).

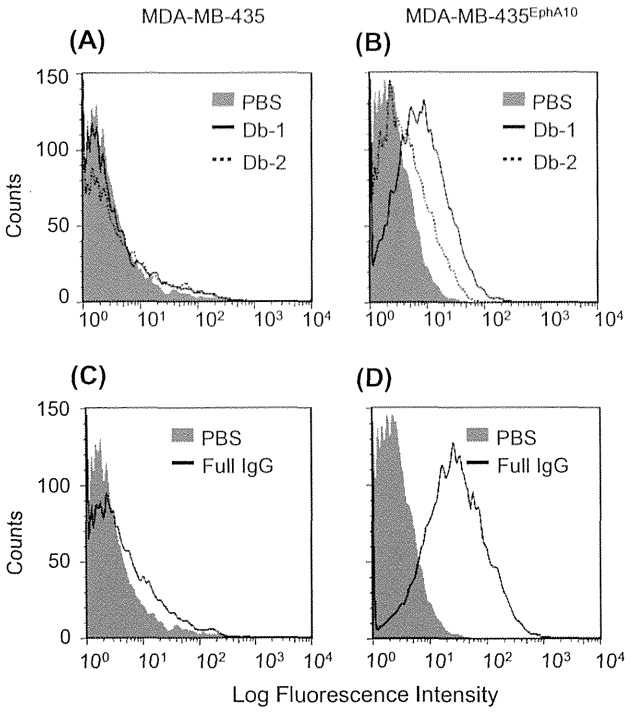

Fig. 3. Binding activity of diabody against EphA10-transfected cells and the parent cells (MDA-MD-435). The left panels (A, C) show the binding ability of the diabodies (A) and of the full IgG (C) against parental cells (MDA-MB-435) and the right panels (B, D) are against EphA10-transfeted cells. Binding activities were measured using 20 μg of each diabody sample. Cell-binding proteins were detected using SureLight P3 conjugated anti-His tag or anti-mouse IgG mAb. Filled bars are vehicle control (PBS).

B, respectively) were constructed (Fig. 1). The plasmid vector construct was designed by adding an N-terminal signal peptide to express BsAb in a soluble form and adding a C-terminal hexahistidine (His × 6) tag or FLAG tag to allow purification by affinity chromatography on a Ni-Sepharose column. This plasmid vector was transfected into BL21 (DE3) Star *E. coli* cells. Pooled supernatants were purified by IMAC using two elution buffers, and fractions containing the diabody further purified by gel-filtration chromatography (Fig. 2A and B). SDS–PAGE under reducing conditions followed by Western blot analysis showed only a single band indicating a ~25 kDa protein (Fig. 2C and D), consistent with the calculated molecular mass of approximately 25 kDa for each scFv. Because these two scFv chains are structured as homodimers, they would be expected to show only low binding activity compared with the heterodimeric form that can fully recognize the target molecules. Therefore, the diabody formulation was checked by western blot against both an anti-His and an anti-FLAG antibody (Fig. 2C and D). These results showed that the diabody existed as heterodimer in the condition of 150 mM imidazole elution, because the amounts of His- and FLAG-tagged scFvs were similar (Fig. 2C). However, the fraction eluted by 300 mM imidazole was primarily composed of homodimers, because the anti-His-tag staining was much stronger than the anti-FLAG tag staining (Fig. 2D). Because His-tagged homodimer antibodies would get trapped strongly by a Ni-Sepharose column, two concentrations of imidazole were used to elute the scFvs (Db-1: 150 mM imidazole/PBS, Db-2: 300 mM imidazole/PBS). The heterodimers indeed were eluted at a lower imidazole concentration than the homodimers.

3.2. Binding activity of diabody for human EphA10

Binding activities of these diabodies (Db-1 and Db-2) were examined by flow cytometric analysis using the MDA-MB-435 parental cells, MDA-MB-435^{EphA10} cells. Specific binding of EphA10 antigens to both Db-1 and Db-2 was observed (Fig. 3). Interestingly, the binding activity of diabody Db-1 was stronger than that of Db-2. These results indicated that the binding activity of the homodimer was reduced because this formulation would have mismatches between each VL and VH. Furthermore, the structural difference between homodimers and heterodimers had a significant effect on the binding activity.

3.3. Redirected target cell lysis of diabody with PBMC

The efficacy of T-cell mediated redirected lysis of MDA-MB-435^{EphA10} cells and the parental cells following addition of each diabody was examined using an LDH cytotoxicity assay. Non-stimulated PBMC were used as effector cells at E/T ratios of 10, respectively. As shown in Fig. 4, the Db-1 and Db-2 diabodies showed dose-dependent cytotoxic activity against MDA-MB-435^{EphA10} cells compared with the scFv constructs (anti-EphA10 scFV). Furthermore, the cytotoxic efficacy of Db-1 was higher than that of Db-2 at low antibody concentrations, indicating that the heterodimer would increase the cytotoxicity related to binding of the antigen.

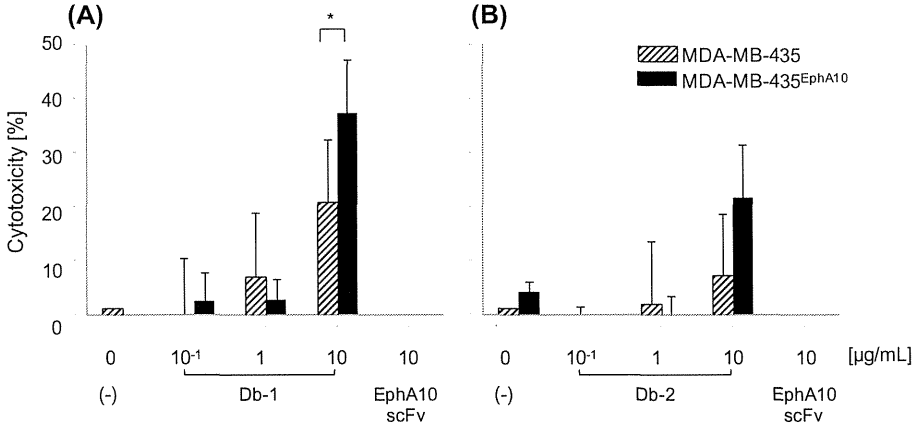

Fig. 4. *In vitro* cytotoxicity of diabody formulations (Db-1 and Db-2) against MDA-MB-435^{EphA10} and parental cells. The left panels are heterodimeric diabody, Db-1 (A) and the right panels are homodimeric diabody, Db-2 (B). MDA-MB-435 parental cells (slashed column) and MDA-MB-435^{EphA10} (black column) cells were co-cultured respectively with human PBMC at E/T ratios of 10. Each point represents the mean of triplicate determinations; error bars represent the standard deviations of triplicate determinations. Asterisks label readings that were statistically significant (unpaired Student's *t*-test) from MDA-MB-435 and MDA-MB-435^{EphA10} ($^*P \leqslant 0.05$).

The results of this study demonstrate that heterodimeric diabodies can show potent binding activity and specificity against cells that express the target antigen. Purified heterodimeric diabody formulations would lead to higher activity because of their increased affinity against two antigens, compared to homodimers or mixtures of homodimers plus heterodimers. Therefore, it is necessary to optimize purification protocols using HPLC etc. However, diabody formulations consisting of two chains of VL and VH could in principle form several types of mixed species. Thus, the protocols for bispecific antibodies should be optimized to produce a formulation containing a single species, e.g. by using linkers to produce a single chain diabody or tandem scFV. This should improve and standardize the desired binding functions of the BsAbs. The construction of such modified antibodies, e.g. scDb and faFV, shows great potential for the development of novel therapeutic drugs.

Acknowledgment

This work was supported by JSPS KAKENHI Grant Number 24680093.

References

[1] H.C. Aasheim, S. Patzke, H.S. Hjorthaug, E.F. Finne, Characterization of a novel Eph receptor tyrosine kinase, EphA10, expressed in testis, Biochim. Biophys. Acta 1723 (2005) 1–7.

[2] L. Truitt, A. Freywald, Dancing with the dead: Eph receptors and their kinase-null partners, Biochem. Cell Biol. 89 (2011) 115–129.

[3] K. Nagano, T. Yamashita, M. Inoue, K. Higashisaka, Y. Yoshioka, Y. Abe, Y. Mukai, H. Kamada, Y. Tsutsumi, S. Tsunoda, Eph receptor A10 has a potential as a target for a prostate cancer therapy, Biochem. Biophys. Res. Commun. 450 (2014) 545–549.

[4] K. Nagano, S. Kanasaki, T. Yamashita, Y. Maeda, M. Inoue, K. Higashisaka, Y. Yoshioka, Y. Abe, Y. Mukai, H. Kamada, Y. Tsutsumi, S. Tsunoda, Expression of Eph receptor A10 is correlated with lymph node metastasis and stage progression in breast cancer patients, Cancer Med. 2 (2013) 972–977.

[5] K. Nagano, Y. Maeda, S. Kanasaki, T. Watanabe, T. Yamashita, M. Inoue, K. Higashisaka, Y. Yoshioka, Y. Abe, Y. Mukai, H. Kamada, Y. Tsutsumi, S. Tsunoda, Ephrin receptor A10 is a promising drug target potentially useful for breast cancers including triple negative breast cancers, J. Control. Release 189 (2014) 72–79.

[6] D. Schrama, R.A. Reisfeld, J.C. Becker, Antibody targeted drugs as cancer therapeutics, Nat. Rev. Drug Discovery 5 (2006) 147–159.

[7] M.K. Gleason, J.A. Ross, E.D. Warlick, T.C. Lund, M.R. Verneris, A. Wiernik, S. Spellman, M.D. Haagenson, A.J. Lenvik, M.R. Litzow, P.K. Epling-Burnette, B.R. Blazar, L.M. Weiner, D.J. Weisdorf, D.A. Vallera, J.S. Miller, CD16xCD33 bispecific killer cell engager (BiKE) activates NK cells against primary MDS and MDSC CD33+ targets, Blood 123 (2014) 3016–3026.

[8] C. Somasundaram, R. Arch, S. Matzku, M. Zoller, Development of a bispecific F(ab')2 conjugate against the complement receptor CR3 of macrophages and a variant CD44 antigen of rat pancreatic adenocarcinoma for redirecting macrophage-mediated tumor cytotoxicity, Cancer Immunol. Immunother. 42 (1996) 343–350.

[9] S.R. Frankel, P.A. Baeuerle, Targeting T cells to tumor cells using bispecific antibodies, Curr. Opin. Chem. Biol. 17 (2013) 385–392.

[10] I. Shimomura, S. Konno, A. Ito, Y. Masakari, R. Orimo, S. Taki, K. Arai, H. Ogata, M. Okada, S. Furumoto, M. Onitsuka, T. Omasa, H. Hayashi, Y. Katayose, M. Unno, T. Kudo, M. Umetsu, I. Kumagai, R. Asano, Rearranging the domain order of a diabody-based IgG-like bispecific antibody enhances its antitumor activity and improves its degradation resistance and pharmacokinetics, MAbs 6 (2014).

[11] R. Asano, T. Kumagai, K. Nagai, S. Taki, I. Shimomura, K. Arai, H. Ogata, M. Okada, F. Hayasaka, H. Sanada, T. Nakanishi, T. Karvonen, H. Hayashi, Y. Katayose, M. Unno, T. Kudo, M. Umetsu, I. Kumagai, Domain order of a bispecific diabody dramatically enhances its antitumor activity beyond structural format conversion: the case of the hEx3 diabody, Protein Eng. Des. Sel. 26 (2013) 359–367.

[12] R. Asano, K. Ikoma, I. Shimomura, S. Taki, T. Nakanishi, M. Umetsu, I. Kumagai, Cytotoxic enhancement of a bispecific diabody by format conversion to tandem single-chain variable fragment (taFv): the case of the hEx3 diabody, J. Biol. Chem. 286 (2011) 1812–1818.

[13] R. Asano, K. Ikoma, Y. Sone, H. Kawaguchi, S. Taki, H. Hayashi, T. Nakanishi, M. Umetsu, Y. Katayose, M. Unno, T. Kudo, I. Kumagai, Highly enhanced cytotoxicity of a dimeric bispecific diabody, the hEx3 tetrabody, J. Biol. Chem. 285 (2010) 20844–20849.

[14] A. Loffler, P. Kufer, R. Lutterbuse, F. Zettl, P.T. Daniel, J.M. Schwenkenbecher, G. Riethmuller, B. Dorken, R.C. Bargou, A recombinant bispecific single-chain antibody, CD19 × CD3, induces rapid and high lymphoma-directed cytotoxicity by unstimulated T lymphocytes, Blood 95 (2000) 2098–2103.

Biochemical and Biophysical Research Communications 450 (2014) 545–549

Contents lists available at ScienceDirect

Biochemical and Biophysical Research Communications

journal homepage: www.elsevier.com/locate/ybbrc

Eph receptor A10 has a potential as a target for a prostate cancer therapy

Kazuya Nagano [a], Takuya Yamashita [a,b], Masaki Inoue [a], Kazuma Higashisaka [a,b], Yasuo Yoshioka [a,b,c], Yasuhiro Abe [d], Yohei Mukai [e], Haruhiko Kamada [a,c], Yasuo Tsutsumi [b,c,e], Shin-ichi Tsunoda [a,b,c,e,*]

[a] Laboratory of Biopharmaceutical Research, National Institute of Biomedical Innovation, 7-6-8 Saito-Asagi, Ibaraki, Osaka 567-0085, Japan
[b] Graduate School of Pharmaceutical Sciences, Osaka University, 1-6 Yamadaoka, Suita, Osaka 565-0871, Japan
[c] The Center of Advanced Medical Engineering and Informatics, Osaka University, 1-6 Yamadaoka, Suita, Osaka 565-0871, Japan
[d] Cancer Biology Research Center, Sanford Research/USD, 2301 E. 60th Street N, Sioux Falls, SD 57104, USA
[e] Laboratory of Innovative Antibody Engineering and Design, National Institute of Biomedical Innovation, 7-6-8 Saito-Asagi, Ibaraki, Osaka 567-0085, Japan

ARTICLE INFO

Article history:
Received 28 May 2014
Available online 9 June 2014

Keywords:
Eph receptor A10
Prostate cancer
Antibody drug

ABSTRACT

We recently identified Eph receptor A10 (EphA10) as a novel breast cancer-specific protein. Moreover, we also showed that an in-house developed anti-EphA10 monoclonal antibody (mAb) significantly inhibited proliferation of breast cancer cells, suggesting EphA10 as a promising target for breast cancer therapy. However, the only other known report for EphA10 was its expression in the testis at the mRNA level. Therefore, the potency of EphA10 as a drug target against cancers other than the breast is not known. The expression of EphA10 in a wide variety of cancer cells was studied and the potential of EphA10 as a drug target was evaluated. Screening of EphA10 mRNA expression showed that EphA10 was overexpressed in breast cancer cell lines as well as in prostate and colon cancer cell lines. Thus, we focused on prostate cancers in which EphA10 expression was equivalent to that in breast cancers. As a result, EphA10 expression was clearly shown in clinical prostate tumor tissues as well as in cell lines at the mRNA and protein levels. In order to evaluate the potential of EphA10 as a drug target, we analyzed complement-dependent cytotoxicity effects of anti-EphA10 mAb and found that significant cytotoxicity was mediated by the expression of EphA10. Therefore, the idea was conceived that the overexpression of EphA10 in prostate cancers might have a potential as a target for prostate cancer therapy, and formed the basis for the studies reported here.

1. Introduction

The development of antibody engineering has enabled a monoclonal antibody (mAb) to become a safe and effective drug for refractory diseases, such as cancer. Today, more than 30 kinds of antibody drugs are approved all over the world. Continued growth in the market is expected in the future [1]. However, the cases to which antibody drugs are applied are limited. Therefore, the development of new antibody drugs is especially needed in the cases without effective treatments, such as a triple negative breast cancer, a castration-resistant prostate cancer, as well as pancreatic cancers or malignant mesotheliomas.

Several Eph receptor family members such as EphA2 or EphB4 are highly expressed in various tumor cell types found in refractory cancers [2], and with expressions associated with tumorigenesis [3,4], proliferation [5,6], vasculogenesis [7,8] and metastasis [9,10]. Therefore, there is a current focus on the development of therapies targeted on Eph members [11]. In this context, MedImmune LLC is developing an antibody-drug conjugate against EphA2 which inhibits tumor growth *in vitro* and *in vivo* [12,13]. It has been tested in phase I to investigate the safety profile and maximum tolerated dose. However, the most recent report announced the trial was stopped halfway due to adverse events such as bleeding and liver disorders [14]. Some databases such as MOPED or PaxDb have reported that EphA2 is highly expressed in platelets and liver tissues. Therefore, the target protein needs to display specific expression in cancer tissues. However, EphA10 which we identified as a novel breast cancer-related protein is hardly expressed in normal human tissues [15] [16]. Furthermore, we also showed that an in-house developed anti-EphA10 mAb inhibited breast cancer cell proliferation at both *in vitro* and *in vivo* levels [16]. These findings

Abbreviations: EphA10, Eph receptor A10; mAb, monoclonal antibody; TMA, tissue microarray; HMEC, human mammary epithelial cell; PrEC, prostate epithelial cell; cDNA, complimentary DNA; FCS, fetal calf serum; PBS, phosphate buffered saline; IHC, immunohistochemistry; CDC, complement-dependent cytotoxicity.

* Corresponding author. Fax: +81 72 641 9817.
E-mail address: tsunoda@nibio.go.jp (S.-i. Tsunoda).

http://dx.doi.org/10.1016/j.bbrc.2014.06.007
0006-291X/

suggest that EphA10 is a promising target for breast cancer therapy. However, the only other known report was that EphA10 is expressed in the testis at the mRNA level [17]. Therefore, the potency of EphA10 as a drug target against cancers other than the breast has not been tested. Here, we report EphA10 expression in various kinds of cancer cells and the potential of EphA10 as a target in other cancer therapies.

2. Material and methods

2.1. Cell lines

The following cancer cell lines were purchased from the American Type Culture Collection (Manassas, VA): HCC70, MDA-MB-157, HCC1599, MDA-MB468, DU4475, 22Rv1, VCaP, colo201, SW620, HCT116, BxPC3, Panc1, AsPC1, H2452, H2052, H28 and Jurkat. The following cancer cell lines were purchased from the Japanese Collection of Research Bioresources Cell Bank (Osaka, Japan): RERF-LC-KJ, RERF-LC-MS, MKN1, MKN45, NEC8, NEC14, A2058, G318, Mewo and K562. PC3 and LNCaP were purchased from the Riken Bioresource Center Cell Bank (Ibaraki, Japan). Normal Human Prostate Epithelial Cells (PrEC) and Normal Human Mammary Epithelial Cells were purchased from Lonza (Basel, Switzerland). All cells were cultured at 37 °C in a humidified atmosphere of 5% CO_2 according to the provider's protocol.

2.2. Real-time PCR

Complementary DNAs (cDNAs) derived from human prostate tumors were purchased from OriGene Technologies (Rockville, MD). The PCR mixture included cDNA template, TaqMan Gene Expression Master Mix and TaqMan probe (EphA10: Hs01017018_m1 or actin-beta: Hs99999903_m1) (Life Technologies, Carlsbad, CA) and the reaction was performed according to the manufacturer's instructions. The threshold cycles were determined using the default settings. EphA10 mRNA expression levels were normalized against actin-beta.

2.3. Cell immunofluorescent staining

PrEC, PC3 and VCaP cells were seeded at 1×10^4 cells/well in Lab-Tek™ 8-well chamber slides (Thermo Fisher Scientific Inc., Waltham, MA). After 24 h, cells were washed twice with PBS, and then fixed with PBS containing 4% paraformaldehyde, pH 8.0 for 10 min. After washing with PBS, fixation was quenched with PBS containing 0.1 M glycine, pH 7.4 for 15 min. Fixed cells were blocked with PBS containing 5% FCS (blocking solution), pH 7.4 for 30 min, and then treated with the anti-EphA10 monoclonal primary antibody and isotype control antibody at 10 μg/ml in blocking solution for 1 h. Donkey anti-mouse IgG conjugated with Alexa Flour 488 (Life Technologies, Carlsbad, CA) was used as the second antibody at 2 μg/ml in the blocking solution for 1 h in the dark. Slides were mounted using a vectashield mounting medium for fluorescence with DAPI (Vector Laboratories Inc., Burlingame, CA) and analyzed with a Leica TCS SP2 confocal laser scanning microscope (Leica Microsystems GmbH, Wetzlar, Germany). Images were further processed using the Adobe Photoshop software.

2.4. Immunohistochemical (IHC) staining

TMAs with prostate tumor and normal prostate tissues (US Biomax, Rockville, MD) were deparaffinized in xylene and rehydrated in a graded series of ethanol. Heat-induced epitope retrieval was performed by maintaining the Target Retrieval Solution (Dako, Glostup, Denmark) by following the manufacturer's instructions. After treatment, endogenous peroxidase was blocked with 0.3%. The TMA slides were incubated with rabbit anti-human EphA10 polyclonal antibody (Abgent Inc., San Diego, CA) for 30 min and then with ENVISION+ Dual Link (Dako, Glostup, Denmark) for 30 min. The reaction products were rinsed three times with 0.05% Tween20/Tris buffer saline and then developed in liquid 3,3′-diaminobenzidine for 3 min. After development, sections were lightly counterstained with Mayer's hematoxylin. All procedures were performed using an AutoStainer (Dako, Glostup, Denmark). Study samples were divided into high and low expression groups based on the two criteria of distribution and quantity. In terms of distribution, the percentage of positive cells across all tumor cells

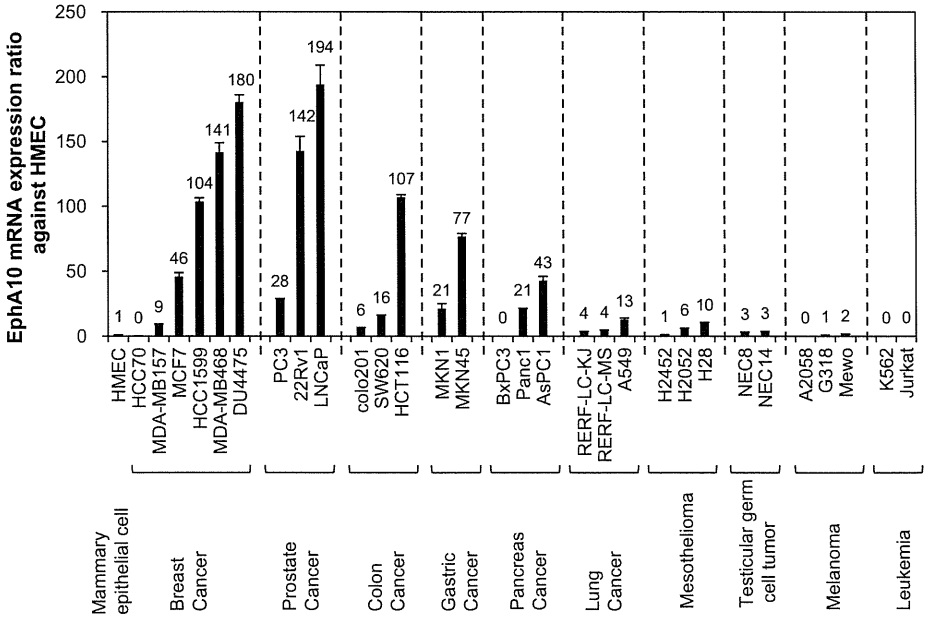

Fig. 1. Screening of EphA10 expression profile in various kinds of cancer cell lines. EphA10 expression in various kinds of cancer cells were screened by quantitative real time PCR. EphA10 expression level in each cell was normalized by actin-beta expression level and described as a ratio against EphA10 expression level in HMEC, normal human mammary epithelial primary cells. $n = 3$ in each group. Error bars represent the SD.

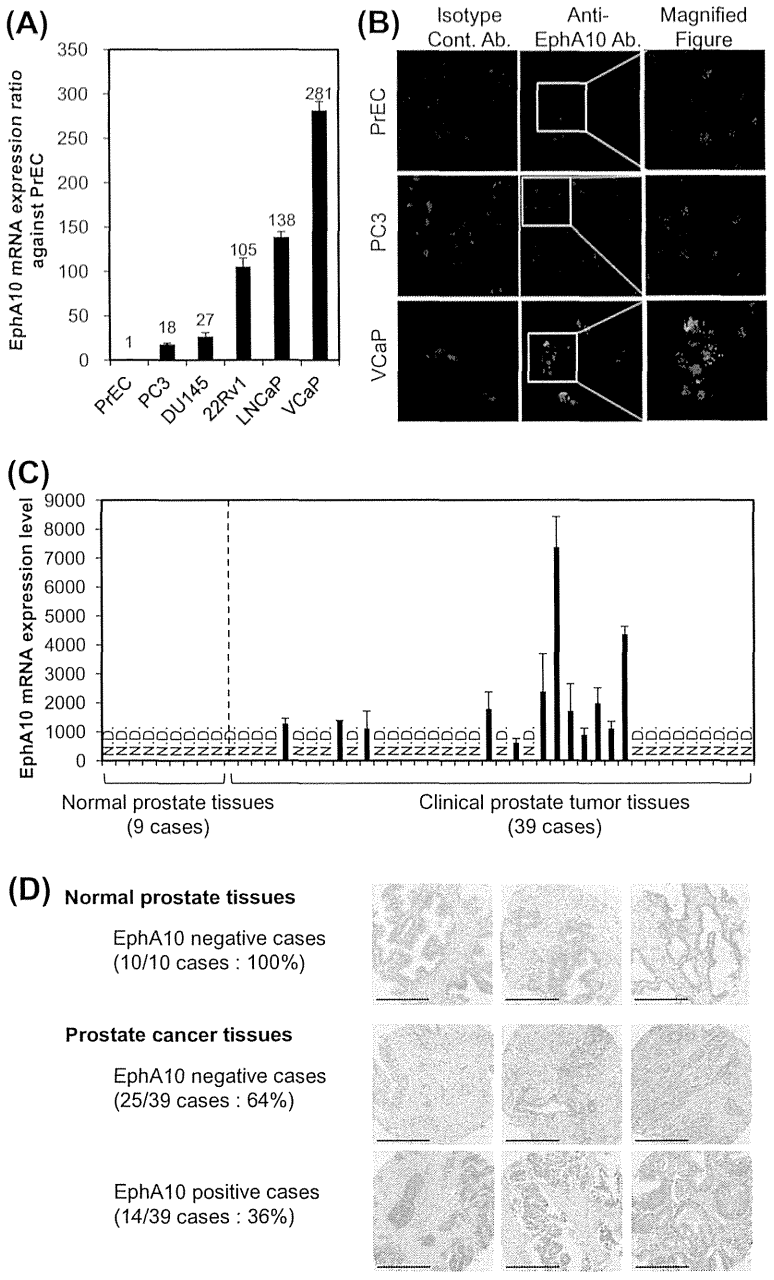

Fig. 2. EphA10 expression analysis in prostate cancer cell lines and clinical prostate cancer tissues at mRNA and protein level. (A) EphA10 mRNA expression level in prostate cancer cell lines (PC3, DU145, 22Rv1, LNCaP and VCaP) was quantified by real time PCR. It was normalized by actin-beta expression level and described as a ratio against EphA10 expression level in PrEC, normal human prostate epithelial primary cells. $n = 3$ in each group. Error bars represent the SD. (B) EphA10 protein expression in prostate cancer cell lines was analyzed by cell immunofluorescent staining. PrEC, PC3 (EphA10-mRNA low expressing cells) and VCaP (EphA10 mRNA high-expressing cells) were treated with anti-EphA10 mAb or the isotype control mAb (20 μg/ml), and then with Alexa Flour 488 conjugated anti-mouse IgG antibody. EphA10 protein expression was detected by confocal microscopy. Blue and green signals relate to DAPI and EphA10, respectively. (C) EphA10 mRNA expression levels in clinical prostate cancer tissues (39 cases) and the normal prostate tissues (9 cases) were quantified in the same method with (A). N.D. means not detectable. (D) TMAs with clinical prostate cancer tissues (39 cases) and the normal tissues (10 cases) were stained using anti-EphA10 mAb. Representative images of normal breast tissue (positive ratio: 0%), EphA10 negative cancer tissue, and EphA10 positive cancer tissues (positive ratio: 36%) are shown. Scale bar: 200 μm.

was scored as 0 (0%), 1 (1–50%), and 2 (51–100%). In terms of quantity, the signal intensity was scored as 0 (no signal), 1 (weak), 2 (moderate) or 3 (marked). Cases with a total score of more than 3 were classified into the high expression group.

2.5. Complement-dependent cytotoxicity (CDC) assay

VCaP cells were seeded at 2×10^4 cells/well in a 96 well cell culture plate (Thermo Fisher Scientific Inc., Waltham, MA) and cultured overnight. After removing the medium, antibodies (anti-EphA10 antibody or the isotype control antibody) and mouse serum as complement were added and incubated for 24 h. Cytotoxicity was evaluated using the WST-8 assay.

3. Results and discussion

3.1. EphA10 mRNA was overexpressed not only in breast cancer cell lines but also in prostate and colon cancer cell lines

In order to screen the types of cancer in which EphA10 is expressed, EphA10 mRNA expression was analyzed not only in breast cancer cells in which we had already shown EphA10

expression, but also in cell lines of colon cancer, gastric cancer, leukemia, lung cancer, melanoma, mesothelioma, pancreas cancer, prostate cancer and testicular germ cell tumors by real time PCR. EphA10 mRNA was expressed by normalizing the actin-beta expression level and represented as the ratio against normal human mammary epithelial primary cells (HMEC). Quantitative analysis demonstrated that EphA10 was expressed not only in breast cancer cells (HCC1599: 103x, MDA-MB468: 141x, DU4475: 181x), but also in prostate cancer cells (22Rv1: 142x, LNCaP: 194x) and colon cancer cells (HCT116: 107x) by more than 100 fold over human mammary epithelial primary cells (HMECs). EphA10 mRNA expression level in breast cancer cell lines was equivalent to that in prostate cancer cell lines (Fig. 1). These data suggested that EphA10 could also be associated with prostate cancers. Therefore, we next focused on prostate cancers and analyzed in more detail the expression of EphA10 at the mRNA and protein levels in cancer cell lines and clinical tissues.

3.2. EphA10 was overexpressed in prostate cancer cell lines and clinical prostate tumor tissues at mRNA and protein level

In order to examine EphA10 expression in prostate cancers, EphA10 expression at the mRNA and protein levels was evaluated in five prostate cancer cell lines (22Rv1, DU145, LNCaP, PC3 and VCaP) and normal human prostate epithelial primary cells (PrECs). Fig. 2(A) shows EphA10 was highly expressed in all cancer cell lines compared to the normal cells. Furthermore, we also analyzed EphA10 expression at the protein level in these cells. Immunofluorescent staining showed that EphA10 expression could not be detected in both PrEC and PC3 (EphA10 mRNA low-expressing cells). On the other hand, EphA10 protein expression was only observed in anti-EphA10 antibody-treated VCaP cells (EphA10 mRNA high-expressing cells), but not in the isotype control antibody-treated VCaP cells (Fig. 2(B)). These data are consistent with the pattern of EphA10 mRNA expression, further demonstrating that EphA10 was overexpressed in prostate cancer cell lines compared to the normal cells.

In order to pursue the overexpression of EphA10 in prostate cancers, we next analyzed EphA10 expression in clinical prostate cancer tissues and in normal prostate tissues. EphA10 expression at the mRNA level was first evaluated using cDNA derived from clinical prostate tumor tissues and the normal prostate tissues. A real time PCR analysis showed that EphA10 mRNA could not be amplified in all 9 normal prostate cases and 27 prostate tumor cases. In contrast, EphA10 expression was observed in 12 prostate tumor cases (approximately 31% in total cases) (Fig. 2(C)). Furthermore, we analyzed the EphA10 protein expression by IHC-staining TMA with clinical prostate cancer tissues and the normal tissues. TMA data showed that EphA10 expression was observed in 14 prostate cancer cases (approximately 36% in total cases), but not in 10 normal prostate tissues and in 25 prostate cancer cases. These data suggested that EphA10 was definitely overexpressed in prostate cancer cell lines as well as in clinical prostate tumor tissues.

We previously showed that EphA10 expression was positively associated with stage progression and lymph node metastasis in clinical breast cancers [18]. Thus, in order to evaluate the role of EphA10 overexpression in prostate cancers, we tried to analyze the relationship between EphA10 expression in clinical prostate cancer tissues and the clinical information such as the size and spread of primary tumor (pT), regional lymph node metastasis (pN), the distant metastasis (pM), and the cancer progression (pStage). Statistical analysis showed that EphA10 expression was not significantly associated with all of the above factors (Supplementary Table S1). It was reported that some Eph receptor members were overexpressed in various kinds of cancers such as breast and prostate [2], and activated by hetero-dimerizing between Eph receptors [19,20]. Therefore, in addition to focusing only on EphA10, analysis of other Eph receptors are needed in order to reveal the role of EphA10 in prostate cancers.

3.3. Anti-EphA10 mAb significantly caused complement-dependent cytotoxicity (CDC) activity dependent on EphA10 expression

In order to evaluate the potential of EphA10 as a target for prostate cancer therapy, we analyzed CDC effects of anti-EphA10 mAb on VCaP cells in which EphA10 was highly expressed. We added anti-EphA10 mAb and mouse serum as complements into VCaP cells and evaluated cytotoxicity on the next day. Fig. 3 shows that cytotoxicity in VCaP was observed only in the co-culture group of anti-EphA10 mAb and mouse serum, but not in the co-culture group of isotype control mAb and mouse serum as well as in mAb alone group. The data indicated that the cytotoxicity of anti-EphA10 mAb was dependent on EphA10 expression, and suggested that EphA10 targeted therapy might be effective in EphA10 positive prostate cancer cases.

Since molecular targeted drugs such as antibody drugs show therapeutic effects related to affinity and specificity for each antigen, it is important that the target protein display enriched expression in cancer tissues. In this respect, we previously reported that EphA10 expression was not observed in almost all normal human organs, except for testis [16]. In order to develop anti-EphA10 mAb therapy and apply it to male patients, EphA10 function in the testis should be analyzed and consider the effects of anti-EphA10 mAb on dysfunction of the testis. On the other hand, many prostate cancer patients are surgically or medically castrated with the purpose of reducing the amount of androgens which promote the growth of prostate cancer cells. However, almost all of the patients have a recurrence which is known as castration-resistant prostate cancer (CRPC). CRPCs are a bottleneck for prostate cancer therapy, because CRPCs have no effective treatment and poor prognosis. Clinical trials of antibody drugs (such as anti-CTLA4 mAb or anti-PD1 mAb) against CRPCs are currently in progress. However the therapeutic effects have been insufficient [21], emphasizing that a novel drug target is urgently needed. In this respect, EphA10 might be a promising target at least for CRPC patients, although further basic experiments are needed such as EphA10 expression analysis in CRPC cases.

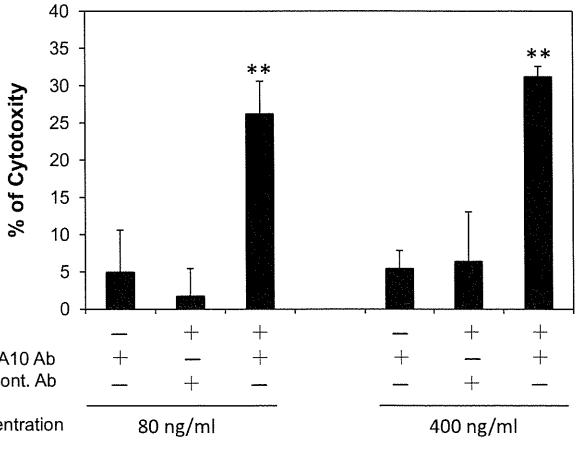

Fig. 3. Complement-dependent cytotoxicity (CDC) effects of anti-EphA10 mAb on VCaP cells. Anti-EphA10 mAb or the isotype control mAb (80 and 400 ng/ml) with/without mouse serum as complements were added to VCaP cells. After 24 h incubation, CDC effects were assessed by WST-8 assay. $^{**}p < 0.01$ vs the isotype control mAb with mouse serum. $n = 3$ in each group. Error bars represent the SD.

In conclusion, we showed that EphA10 was overexpressed in prostate cancers and suggest that EphA10 is a potential target for prostate cancer therapy.

Conflict of interest statement

The authors have no conflict of interest.

Acknowledgments

This study was supported in part by Grants-in-Aid for Scientific Research from the Project for Development of Innovative Research on Cancer Therapeutics, the Ministry of Education, Culture, Sports, Science and Technology of Japan, and from the Japan Society for the Promotion of Science. This study was also supported in part by Health Labor Sciences Research Grants from the Ministry of Health, Labor and Welfare of Japan.

Appendix A. Supplementary data

Supplementary data associated with this article can be found, in the online version, at http://dx.doi.org/10.1016/j.bbrc.2014.06.007.

References

[1] A.L. Nelson, E. Dhimolea, J.M. Reichert, Development trends for human monoclonal antibody therapeutics, Nat. Rev. Drug Discov. 9 (2010) 767–774.
[2] H.Q. Xi, X.S. Wu, B. Wei, L. Chen, Eph receptors and ephrins as targets for cancer therapy, J. Cell. Mol. Med. 16 (2012) 2894–2909.
[3] D.M. Brantley-Sieders, G. Zhuang, D. Hicks, W.B. Fang, Y. Hwang, J.M. Cates, K. Coffman, D. Jackson, E. Bruckheimer, R.S. Muraoka-Cook, J. Chen, The receptor tyrosine kinase EphA2 promotes mammary adenocarcinoma tumorigenesis and metastatic progression in mice by amplifying ErbB2 signaling, J. Clin. Invest. 118 (2008) 64–78.
[4] N. Munarini, R. Jager, S. Abderhalden, G. Zuercher, V. Rohrbach, S. Loercher, B. Pfanner-Meyer, A.C. Andres, A. Ziemiecki, Altered mammary epithelial development, pattern formation and involution in transgenic mice expressing the EphB4 receptor tyrosine kinase, J. Cell. Sci. 115 (2002) 25–37.
[5] S.R. Kumar, J. Singh, G. Xia, V. Krasnoperov, L. Hassanieh, E.J. Ley, J. Scehnet, N.G. Kumar, D. Hawes, M.F. Press, F.A. Weaver, P.S. Gill, Receptor tyrosine kinase EphB4 is a survival factor in breast cancer, Am. J. Pathol. 169 (2006) 279–293.
[6] K.A. Mohammed, X. Wang, E.P. Goldberg, V.B. Antony, N. Nasreen, Silencing receptor EphA2 induces apoptosis and attenuates tumor growth in malignant mesothelioma, Am. J. Cancer Res. 1 (2011) 419–431.
[7] N.K. Noren, M. Lu, A.L. Freeman, M. Koolpe, E.B. Pasquale, Interplay between EphB4 on tumor cells and vascular ephrin-B2 regulates tumor growth, Proc. Natl. Acad. Sci. U.S.A. 101 (2004) 5583–5588.
[8] S. Sawamiphak, S. Seidel, C.L. Essmann, G.A. Wilkinson, M.E. Pitulescu, T. Acker, A. Acker-Palmer, Ephrin-B2 regulates VEGFR2 function in developmental and tumour angiogenesis, Nature 465 (2010) 487–491.
[9] D.M. Brantley-Sieders, W.B. Fang, D.J. Hicks, G. Zhuang, Y. Shyr, J. Chen, Impaired tumor microenvironment in EphA2-deficient mice inhibits tumor angiogenesis and metastatic progression, FASEB J. 19 (2005) 1884–1886.
[10] X.D. Ji, G. Li, Y.X. Feng, J.S. Zhao, J.J. Li, Z.J. Sun, S. Shi, Y.Z. Deng, J.F. Xu, Y.Q. Zhu, H.P. Koeffler, X.J. Tong, D. Xie, EphB3 is overexpressed in non-small-cell lung cancer and promotes tumor metastasis by enhancing cell survival and migration, Cancer Res. 71 (2011) 1156–1166.
[11] A.W. Boyd, P.F. Bartlett, M. Lackmann, Therapeutic targeting of EPH receptors and their ligands, Nat. Rev. Drug Discov. 13 (2014) 39–62.
[12] D. Jackson, J. Gooya, S. Mao, K. Kinneer, L. Xu, M. Camara, C. Fazenbaker, R. Fleming, S. Swamynathan, D. Meyer, P.D. Senter, C. Gao, H. Wu, M. Kinch, S. Coats, P.A. Kiener, D.A. Tice, A human antibody-drug conjugate targeting EphA2 inhibits tumor growth in vivo, Cancer Res. 68 (2008) 9367–9374.
[13] J.W. Lee, R.L. Stone, S.J. Lee, E.J. Nam, J.W. Roh, A.M. Nick, H.D. Han, M.M. Shahzad, H.S. Kim, L.S. Mangala, N.B. Jennings, S. Mao, J. Gooya, D. Jackson, R.L. Coleman, A.K. Sood, EphA2 targeted chemotherapy using an antibody drug conjugate in endometrial carcinoma, Clin. Cancer Res. 16 (2010) 2562–2570.
[14] C.M. Annunziata, E.C. Kohn, P. LoRusso, N.D. Houston, R.L. Coleman, M. Buzoianu, G. Robbie, R. Lechleider, Phase 1, open-label study of MEDI-547 in patients with relapsed or refractory solid tumors, Invest. New Drugs 31 (2013) 77–84.
[15] S. Imai, K. Nagano, Y. Yoshida, T. Okamura, T. Yamashita, Y. Abe, T. Yoshikawa, Y. Yoshioka, H. Kamada, Y. Mukai, S. Nakagawa, Y. Tsutsumi, S. Tsunoda, Development of an antibody proteomics system using a phage antibody library for efficient screening of biomarker proteins, Biomaterials 32 (2011) 162–169.
[16] K. Nagano, Y. Maeda, S. Kanasaki, T. Watanabe, T. Yamashita, M. Inoue, K. Higashisaka, Y. Yoshioka, Y. Abe, Y. Mukai, H. Kamada, Y. Tsutsumi, S. Tsunoda, Ephrin receptor A10 is a promising drug target potentially useful for breast cancers including triple negative breast cancers, J. Control Release, in press.
[17] H.C. Aasheim, S. Patzke, H.S. Hjorthaug, E.F. Finne, Characterization of a novel Eph receptor tyrosine kinase, EphA10, expressed in testis, Biochim. Biophys. Acta 1723 (2005) 1–7.
[18] K. Nagano, S. Kanasaki, T. Yamashita, Y. Maeda, M. Inoue, K. Higashisaka, Y. Yoshioka, Y. Abe, Y. Mukai, H. Kamada, Y. Tsutsumi, S. Tsunoda, Expression of Eph receptor A10 is correlated with lymph node metastasis and stage progression in breast cancer patients, Cancer Med. 2 (2013) 972–977.
[19] B.P. Fox, R.P. Kandpal, A paradigm shift in EPH receptor interaction: biological relevance of EPHB6 interaction with EPHA2 and EPHB2 in breast carcinoma cell lines, Cancer Genomics Proteomics 8 (2011) 185–193.
[20] A. Freywald, N. Sharfe, C.M. Roifman, The kinase-null EphB6 receptor undergoes transphosphorylation in a complex with EphB1, J. Biol. Chem. 277 (2002) 3823–3828.
[21] S.L. Topalian, F.S. Hodi, J.R. Brahmer, S.N. Gettinger, D.C. Smith, D.F. McDermott, J.D. Powderly, R.D. Carvajal, J.A. Sosman, M.B. Atkins, P.D. Leming, D.R. Spigel, S.J. Antonia, L. Horn, C.G. Drake, D.M. Pardoll, L. Chen, W.H. Sharfman, R.A. Anders, J.M. Taube, T.L. McMiller, H. Xu, A.J. Korman, M. Jure-Kunkel, S. Agrawal, D. McDonald, G.D. Kollia, A. Gupta, J.M. Wigginton, M. Sznol, Safety, activity, and immune correlates of anti-PD-1 antibody in cancer, N. Engl. J. Med. 366 (2012) 2443–2454.

Journal of Controlled Release 189 (2014) 72–79

Contents lists available at ScienceDirect

Journal of Controlled Release

journal homepage: www.elsevier.com/locate/jconrel

Ephrin receptor A10 is a promising drug target potentially useful for breast cancers including triple negative breast cancers

Kazuya Nagano [a], Yuka Maeda [a,b], So-ichiro Kanasaki [a,b], Takanobu Watanabe [a,b], Takuya Yamashita [a,b], Masaki Inoue [a], Kazuma Higashisaka [a,b], Yasuo Yoshioka [a,b,c], Yasuhiro Abe [a], Yohei Mukai [d], Haruhiko Kamada [a,c], Yasuo Tsutsumi [b,c], Shin-ichi Tsunoda [a,b,c,*]

[a] Laboratory of Biopharmaceutical Research, National Institute of Biomedical Innovation, 7-6-8 Saito-Asagi, Ibaraki, Osaka 567-0085, Japan
[b] Graduate School of Pharmaceutical Sciences, Osaka University, 1-6 Yamadaoka, Suita, Osaka 565-0871, Japan
[c] The Center of Advanced Medical Engineering and Informatics, Osaka University, 1-6 Yamadaoka, Suita, Osaka 565-0871, Japan
[d] Laboratory of Innovative Antibody Engineering and Design, National Institute of Biomedical Innovation, 7-6-8 Saito-Asagi, Ibaraki, Osaka 567-0085, Japan

ARTICLE INFO

Article history:
Received 31 March 2014
Accepted 9 June 2014
Available online 16 June 2014

Keywords:
Ephrin receptor A10
Antibody drug
Triple negative breast cancer
Cell proliferation

ABSTRACT

Ephrin receptor A10 (EphA10) is a relatively uncharacterized protein which is expressed in many breast cancers but not expressed in normal breast tissues. Here, we examined the potential of EphA10 as a drug target in breast cancer. Immunohistochemical staining of clinical tissue sections revealed that EphA10 was expressed in various breast cancer subtypes, including triple negative breast cancers (TNBCs), with no expression observed in normal tissues apart from testis. Ligand-dependent proliferation was observed in EphA10-transfected MDA-MB-435 cells (MDA-MB-435^{EphA10}) and native TNBC cells (MDA-MB-436). However, this phenomenon was not observed in parental MDA-MB-435 cells which express a low level of EphA10. Finally, tumor growth was significantly suppressed by administration of an anti-EphA10 monoclonal antibody in a xenograft mouse model. These results suggest that inhibition of EphA10 signaling may be a novel therapeutic option for management of breast cancer, including TNBCs which are currently not treated with molecularly targeted agents.

1. Introduction

Expression of the estrogen receptor (ER), progesterone receptor (PR) and Her2 in breast cancer tissues is an important indicator in determining treatment options against the disease [1,2]. Anti-hormone therapies and anti-Her2 therapies such as tamoxifen and trastuzumab are chosen against ER/PR positive cases and Her2 positive cases, respectively [1,2]. However, triple negative breast cancer (TNBC), which lacks expression of ER, PR and Her2, is known to be refractory due to absence of molecularly targeted drugs [3–5]. Therefore, there is considerable interest worldwide in respect to the development of therapeutics against TNBC.

Ephrin receptor superfamily members are subdivided into nine type A molecules (EphA1–A8, A10) and five type B molecules (EphB1–B4, B6) in mammals [6,7]. Several Eph members such as EphA2 or EphB4 are overexpressed in various tumor cell types [8,9], with expression also related to tumorigenesis [10–12], proliferation [13,14], vasculogenesis [15–17] and metastasis [18–20]. There is a current focus on the development of Eph member-targeted therapies. In this context, an antibody-drug conjugate against EphA2 is being developed by MedImmune LLC which inhibits tumor growth *in vitro* and *in vivo*[21–23] and has been tested in phase I to investigate the safety profile and maximum tolerated dose. However, the most recently reported phase I results show that the trial study was stopped halfway due to adverse events such as bleeding and liver disorders [24]. Certainly, it is reported in some databases such as MOPED or PaxDb that EphA2 is highly expressed in platelet and liver tissues. As antibody-based drugs show therapeutic effects related to affinity and specificity for the respective antigen, the target protein needs to display enriched expression in cancer tissues.

Against this background, we had identified EphA10 as being expressed in many breast cancer tissues, but not in normal breast tissues, using an antibody proteomics system [25]. EphA10 is a relatively uncharacterized protein. The only finding known before our report was that EphA10 is expressed in the testis at mRNA level [26]. Therefore, EphA10 is a highly novel breast cancer-related protein. However, the expression profile of EphA10 protein in normal and cancer tissues, as well as function, must be clarified in order to determine its potential as a drug target.

Here, we firstly showed EphA10 expression in various breast cancer cases, including TNBC, with no expression observed in normal tissues apart from testis. Furthermore, we investigated the potency of EphA10 targeted therapy through the use of an anti-EphA10 monoclonal antibody (mAb).

* Corresponding author at: Laboratory of Biopharmaceutical Research, National Institute of Biomedical Innovation, 7-6-8 Saito-Asagi, Ibaraki, Osaka 567-0085, Japan. Tel.: +81 72 641 9814; fax: +81 72 641 9817.
E-mail address: tsunoda@nibio.go.jp (S. Tsunoda).

http://dx.doi.org/10.1016/j.jconrel.2014.06.010
0168-3659/

2. Material and methods

2.1. Cell lines and culture

MDA-MB-435 and MDA-MB-436 cells were obtained from the American Type Culture Collection (ATCC, Manassas, VA). Both cells were cultured in Dulbecco's modified eagle medium (DMEM) with 10% fetal calf serum (FCS). Stably expressing EphA10 transfectant cells (MDA-MB-435^{EphA10}) were established in our laboratory. In brief, lentiviral particles encoding human EphA10 were prepared using 293T cells (ATCC, Manassas, VA) and infected into MDA-MB-435 cells at a multiplicity of infection of 100. Stable EphA10 transfectants were selected and maintained for growth in 10% FCS/DMEM medium containing 8 μg/ml blasticidin. All cells were cultured at 37 °C in a humidified atmosphere of 5% CO_2.

2.2. BrdU incorporation assay

MDA-MB-435, MDA-MB-435^{EphA10} and MDA-MB-436 cells were seeded at 5×10^3 cells/well in a 96-well cell culture plate and incubated overnight. After 24 h ofstarvation in medium without FCS, EphrinA3-Fc, EphrinA4-Fc and EphrinA5-Fc chimera recombinant proteins (R&D Systems Inc., Minneapolis, MN) or anti-EphA10 mAb were added and incubated for 12 h. Cell proliferation was evaluated using a dedicated ELISA kit which measures BrdU incorporation (Roche Applied Science, Penzberg, Germany). For this assay, BrdU solution was added to those cells being stimulated with EphA10 ligand and incubated for 2 h. After cell fixation, POD-labeled anti-BrdU antibody was added and incubated at RT for 90 min. After three washes, the level of BrdU incorporation was determined by adding the substrate.

2.3. Development of anti-EphA10 mAb

BALB/c mice were immunized with EphA10-Fc chimera recombinant protein (R&D Systems Inc., Minneapolis, MN) four times. After the antibody titers for EphA10 were shown to be optimal by ELISA, hybridoma cells were obtained by fusion of myeloma cells with immunized spleen cells in the usual manner. Positive clones for EphA10 binding were selected by flow cytometry and ELISA methods.

2.4. Affinity evaluation as determined by surface plasmon resonance (SPR)

Protein interactions were evaluated using a BIAcore3000 system (GE Healthcare Bio-Sciences AB, Uppsala, Sweden). Anti-EphA10 mAb or each EphA10 ligand (EphrinA3-Fc, EphrinA4-Fc and EphrinA5-Fc) was mixed in series of combinations with EphA10-Fc chimera recombinant protein immobilized on a sensor chip CM5. The kinetic parameters of these interactions were calculated using a single- or multi-cycle kinetic analysis method.

2.5. Tumor accumulation analysis of anti-EphA10 mAb

Alexa Fluor 647-labeled Anti-EphA10 mAb or IgG2b isotype control mAb was intravenously administered into xenograft mouse models bearing MDA-MB-435^{EphA10} or MDA-MB-435 at 200 μg/mouse. The mice were then imaged daily (24–96 h) and associated fluorescent intensity was measured using the OV110 *in vivo* observation system (Olympus Corp., Tokyo, Japan). Tumor accumulation was quantified as the ratio of mean fluorescent intensity in tumors compared to that observed on the contralateral side skin. After 96 h of administration, tumor tissues were isolated from dissected mice, and their mean fluorescent intensity was measured.

2.6. Anti-EphA10 mAb treatment in a mouse xenograft model

A xenograft mouse model was constructed by orthotopic transplantation of MDA-MB-435^{EphA10}. When the tumor size reached approximately 100 mm^3, saline, anti-EphA10 mAb and control mAb were intraperitoneally administered twice a week (1 mg/mouse or 0.5 mg/mouse) or intravenously administered once a week (0.4 mg/mouse or 0.2 mg/mouse). Tumor volume was assessed over time using the following formula – tumor volume = $LW^2/2$, where L is long diameter and W is the short diameter. At day 47 (intraperitoneal administration) or day 53 (intravenous administration), tumor tissues were isolated from dissected mice, and their weights measured.

2.7. Statistical methods

All analyses were performed using GraphPad Prism 5 version (GraphPad Software Inc., La Jolla, CA). Student *t* test or one-way ANOVA test was used to compare the two or multiple groups, respectively. All hypothesis testing were two-tailed with a significance level of <0.05.

3. Results

3.1. EphA10 was expressed in various subtypes of breast tumors, but not in many types of normal tissues

We previously showed that EphA10 is preferentially expressed in breast cancer compared to normal breast tissues. However, the expression profile of EphA10 has not been examined in relation to the various subtypes of breast cancer as yet. Breast cancer patients are divided into the following four therapeutically-relevant subtypes on the basis of Her2, ER and PR expressions in tumor cells: luminal A (Her2 −, ER + and/or PR +), luminal B (Her2 +, ER + and/or PR +), Her2-enriched (Her2 +, ER −, PR −) and TNBC (Her2 −, ER −, PR −) [1,27]. In order to comprehensively evaluate the utility of EphA10 as a drug target in breast cancer, we firstly analyzed its expression profile within the above-mentioned subtypes using tissue microarray (TMA) technology. As determined by immunohistochemical (IHC) staining, EphA10 was seen to be specifically expressed in cancer cells from each subtype (Fig. S1 (A)). Moreover, assessment of staining images indicated that the proportion of EphA10-positive tumors per subtype was as follows: luminal A (54%), luminal B (68%), Her2-enriched (64%) and TNBC (67%) (Table 1). These data suggest EphA10 as an attractive target in breast cancer, particularly in relation to patients with TNBC which is under-served by current molecularly targeted drugs.

In order to evaluate the specificity of EphA10 expression, we next analyzed EphA10 protein levels in 36 types of normal tissues. IHC analysis of a normal human organ TMA showed EphA10 to be expressed in testis tissues (Fig. S1 (B)). However, EphA10 expression was not

Table 1
EphA10 expression profile in four subtypes of breast cancer.

	Positive cases(ratio)		Negative cases (ratio)		Total cases
Luminal A	22	(54%)	19	(46%)	41
Luminal B	25	(68%)	12	(32%)	37
Her2-enriched	16	(64%)	11	(36%)	27
TNBC	10	(67%)	5	(33%)	15
Total cases	73	(61%)	47	(39%)	120

Table 2
Expression profile of EphA10 in various types of normal tissues.

Tissue	Positive cases (ratio)		Tissue	Positive cases (ratio)	
Adrenal grand	0/3	(0%)	Nerve	0/3	(0%)
Bladder	0/3	(0%)	Ovary	0/3	(0%)
Bone marrow	0/3	(0%)	Pancreas	0/3	(0%)
Breast	0/3	(0%)	Parathyroid gland	0/3	(0%)
Cerebellum	0/3	(0%)	Pituitary	0/3	(0%)
Cerebral gray matter	0/3	(0%)	Prostate	0/3	(0%)
Cerebral white matter	0/3	(0%)	Salivary gland	0/3	(0%)
Colon	0/3	(0%)	Skeletal muscle	0/3	(0%)
Esophagus	0/3	(0%)	Skin	0/3	(0%)
Eye	0/3	(0%)	Small intestine	0/3	(0%)
Head and neck	0/3	(0%)	Spleen	0/3	(0%)
Heart	0/3	(0%)	Stomach	0/3	(0%)
Kidney	0/3	(0%)	Testis	3/3	(100%)
Larynx	0/3	(0%)	Thymus gland	0/3	(0%)
Liver	0/3	(0%)	Thyroid	0/3	(0%)
Lung	0/3	(0%)	Tonsil	0/3	(0%)
Lymph node	0/3	(0%)	Uterine cervix	0/3	(0%)
Mesothelium	0/3	(0%)	Uterus	0/3	(0%)

observed in the other 35 kinds of normal tissues tested (Table 2). Moreover, we also confirmed the testis-specific expression profile of EphA10 at the mRNA level *via* real-time quantitative PCR methods (Fig. S2). Although a modest degree of EphA10 mRNA expression was detected in colon, kidney and small intestine tissues, this was not observed at the protein level by IHC staining (Table 2 and Fig. S1 (B)). These data suggested that EphA10 is a highly specific tumor antigen. Therefore, EphA10 is a potentially useful target for breast cancer including TNBC on the basis of particular expression profiles.

3.2. Cell proliferation was promoted by EphA10 ligand stimulation and inhibited by co-addition of anti-EphA10 mAb in vitro

Clarifying the role of EphA10 in cancer is essential for the development of safe and effective drugs targeting this protein. In order to analyze its function in breast cancer, we generated cell lines ectopically overexpressing EphA10 and compared the phenotype of these cells *versus* the corresponding parental line. For this, we infected EphA10-encoding lentiviral particles into MDA-MB-435 cells (which express a low level of EphA10), generating transduced cells stably overexpressing EphA10 (MDA-MB-435^{EphA10}) (Fig. S3 (A)). The expression level of EphA10 observed in certain clinical breast tumor tissues was similar to that seen in MDA-MB-435^{EphA10} cells (Fig. S3 (B)), suggesting that the transduced cells were suitable for functional analysis of EphA10 *in vitro*. In order to analyze the effects of EphA10 signaling on tumor cell proliferation, a key hallmark of malignancy, we compared the rates of BrdU incorporation (a measure of DNA synthesis) between MDA-MB-435^{EphA10} and parental cells following stimulation with the EphA10 ligands, EphrinA3, EphrinA4 and EphrinA5. Addition of the ligands to both cell lines significantly induced BrdU incorporation in a dose-dependent manner in MDA-MB-435^{EphA10} cells as compared to MDA-MB-435 cells (Fig. 1(A) and (B)). Next, we evaluated the proliferative activity of breast cancer cells that endogenously express EphA10. We examined EphA10 expression levels in three different breast cancer cell lines by quantitative RT-PCR assay and found that MDA-MB-436, TNBC cells, contained a moderate level of endogenous EphA10 (Fig. S4). Thus, we also performed a BrdU incorporation assay with EphrinA3, A4 and A5. As a result, Ephrin-dependent proliferation was also observed in MDA-MB-436 cells (Fig. 1(C)). Furthermore, we also confirmed the positive effects on proliferation mediated by EphA10 signaling in MDA-MB-436 cells *via* WST-8 assay (data not shown). These data suggested that EphA10 signaling may promote proliferation of breast cancer cells.

In order to analyze the phenomenon in detail, we generated a first-in-kind inhibitory anti-EphA10 mAb. Binding affinity studies showed that mAb specifically bound to EphA10, but not to eight other EphA family proteins (Fig. S5 (A)). Moreover, SPR analysis indicated that the mAb displayed an affinity against EphA10 in the nanomolar range (KD = 1.9 nM) (Fig. S5 (B)). Furthermore, flow cytometric analysis showed that the mAb reacted with MDA-MB-435^{EphA10} but not with parental cells (Fig. S5 (C)). These data suggested that the anti-EphA10 mAb had high specificity and affinity towards its target, equivalent to that of existing antibody-based drugs such as trastuzumab (KD = 1–5 nM) and bevacizumab (KD = 1.1 nM).

In order to evaluate the potential inhibitory effect on EphA10 signaling, we added the anti-EphA10 mAb to the BrdU incorporation assay. As a result, the rate of BrdU incorporation was significantly inhibited in a group co-treated with EphA10 ligands and anti-EphA10 mAb in EphA10 transfectant cells (MDA-MB-435^{EphA10}) (Fig. 1(D)–(F)) and native TNBC cells (MDA-MB-436) (Fig. 1(G)–(I)). Consequently, inhibition of EphA10 signaling *via* this antibody suppressed ligand-dependent stimulation of tumor cell proliferation. These findings suggested that EphA10 targeted therapy might have significant potency in a breast cancer context.

3.3. Proliferation induced by EphA10 signaling may be mediated by p38 phosphorylation

In order to analyze the molecular mechanism underlying EphA10-mediated proliferation, we focused on the mitogen-activated protein kinase (MAPK) pathway, which is centrally involved in regulating cell proliferation. In the case of many growth factor receptors, such as epidermal growth factor receptor or vascular endothelial growth factor receptor, cell proliferation is caused by promoting the phosphorylation of Erk1/2 [28–30]. Moreover, in some receptor classes, such as transforming growth factor receptor or fibroblast growth factor receptor, cell proliferation is caused by promoting the phosphorylation of p38 [31,32]. Therefore, we compared the phosphorylation of Erk1/2 or p38 in MDA-MB-435^{EphA10} and parental cells following stimulation with EphA10 ligands. Western blotting analysis showed that the degree of phosphorylated Erk1/2 in both cell types essentially unchanged following exposure to any of the EphA10 ligands (Fig. S6 (A)). Next, we compared the extent of phosphorylated p38 between EphA10-overexpressing and parental MDA-MB-435 cells. In this context, the level of phosphorylated p38 in parental MDA-MB-435 cells was practically unchanged in response to any of the EphA10 ligands. On the other hand, phosphorylated p38 levels in MDA-MB-435^{EphA10} cells tended to be elevated following stimulation with EphrinA3, A4 and A5 (Fig. S6 (B)). In order to reveal the relationship of p38 phosphorylation to Ephrin-mediated effects on cell proliferation, we analyzed BrdU

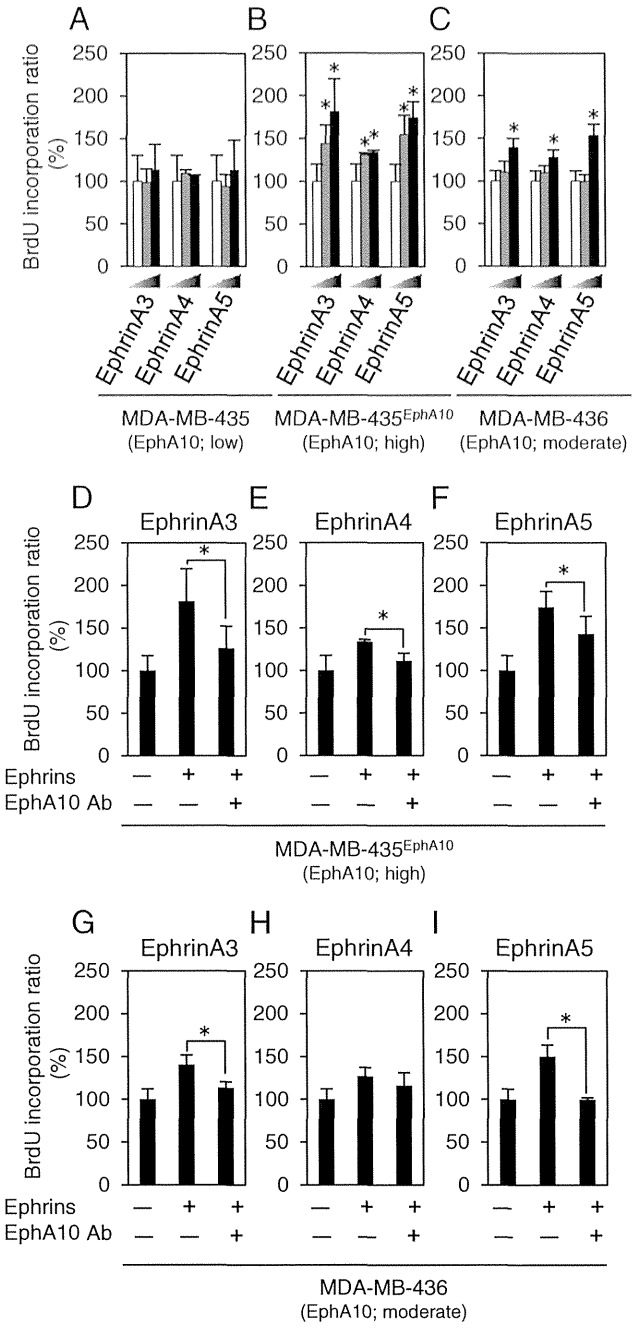

Fig. 1. BrdU incorporation analysis in relation to EphA10 signaling. After incubation of EphrinA3-Fc, EphrinA4-Fc or EphrinA5-Fc at a series of concentrations (white, gray or black bars indicate 0, 0.25, 4 μg/ml, respectively) with (A) MDA-MB-435, (B) MDA-MB-435^{EphA10} or (C) MDA-MB-436 cells for 12 h, cell proliferation mediated by EphA10 was evaluated by measuring the rate of BrdU incorporation (*: $p < 0.05$ *vs* non-treatment group, one-way ANOVA). Moreover, (D) (G) EphrinA3-Fc, (E) (H) EphrinA4-Fc and (F) (I) EphrinA5-Fc (4 μg/ml) and/or anti-EphA10 mAb (20 μg/ml) were incubated with (D)–(F) MDA-MB-435^{EphA10} or (G)–(I) MDA-MB-436 cells for 12 h. Cell proliferation and inhibition effects were analyzed as before (*: $p < 0.05$ *vs* EphA10 ligand only group, one-way ANOVA). Error bars indicate the mean + S.D. (n = 4–6).

Table 3
Kinetic parameters of the interaction between EphA10 and its ligands.

	ka (M^{-1} s^{-1})	kd (s^{-1})	KD (M)
EphrinA3	1.3×10^{6}	1.9×10^{-3}	1.4×10^{-9}
EphrinA4	3.7×10^{5}	1.4×10^{-3}	3.8×10^{-9}
EphrinA5	1.0×10^{6}	9.2×10^{-4}	8.9×10^{-10}

Indication of each kinetic parameter is as follows.
ka: association rate constant.
kd: dissociation rate constant.
KD: equilibrium dissociation constant.

incorporation following Ephrin exposure plus/minus a p38 inhibitor (SB203580). The results showed that the rate of BrdU incorporation was significantly inhibited in cells co-treated with the p38 inhibitor (Fig. S6 (C)). These data suggested that cell proliferation by EphA10 signaling may be mediated *via* p38 phosphorylation.

3.4. Affinity of EphA10 ligands, EphrinA3, A4 and A5 against EphA10

It has previously been reported that EphrinA3, A4 and A5 bind as ligands to EphA10 [26]. However, the affinities of these ligands for EphA10 have not been clarified as yet. In order to evaluate the potential difference in signal transduction activities caused by stimulation of

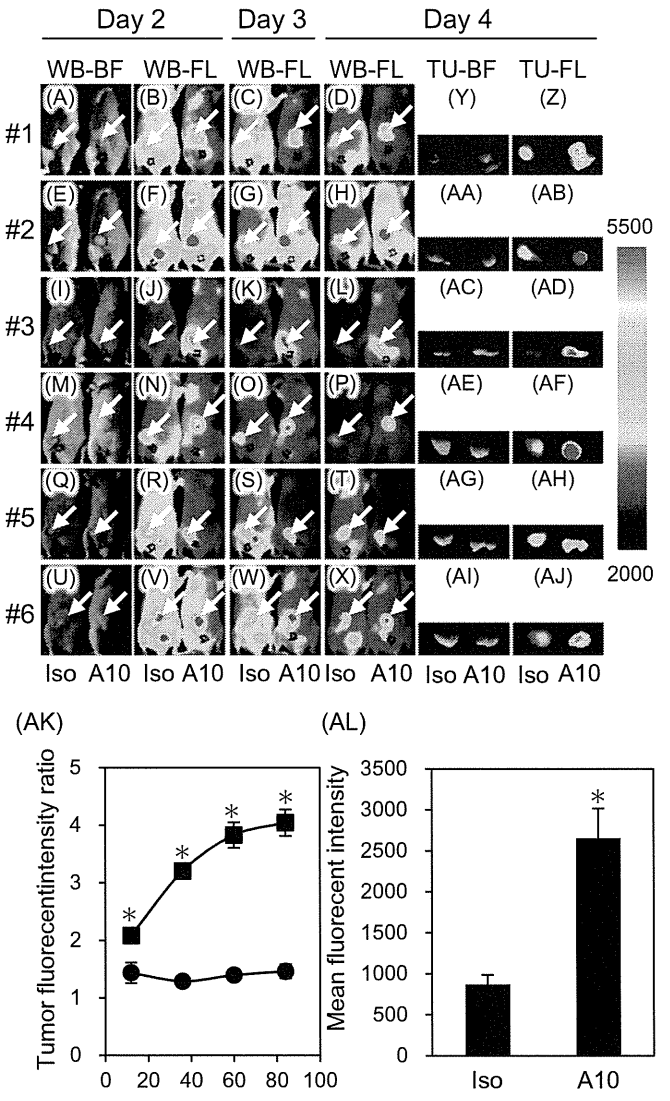

Fig. 2. *In vivo* biodistribution of anti-EphA10 mAb in a xenograft mouse model. Alexa Fluor 647-labeled anti-EphA10 mAb or an isotype control mAb was intravenously administered (200 μg/mouse) into a xenograft mouse model carrying EphA10-expressing tumors (n = 6). (A)–(X) Fluorescence was observed on a daily basis using a whole animal imaging system. The panel on the extreme left and the adjacent panels are brightfield (day 2) and fluorescent (day 2, 3 and 4) images, respectively. The left- and right-hand mice in each image were treated with Alexa Fluor 647-labeled control mAb and anti-EphA10 mAb, respectively. Arrows in each image indicate location of tumor tissues. WB, BF, FL and TU in the upper panel indicate whole body, brightfield, fluorescence and tumor tissue, respectively. Iso and A10 indicate Alexa Fluor 647-labeled isotype control mAb treated mice and Alexa Fluor 647-labeled anti-EphA10 mAb treated mice, respectively. (Y)–(AJ) At day 4, tumor tissues were isolated from dissected mice, with associated fluorescence measured. The left- and right-hand panels are brightfield and fluorescent images of the tumor tissues, respectively. The right-hand bar chart indicates fluorescent intensity range. (AK) Tumor accumulation of anti-EphA10 mAb (■) and the control mAb (●) was quantified as the ratio of fluorescence intensity observed at the tumor over that seen at the contralateral site skin. $^{*}p < 0.05$ (*t*-test). (AL) Mean fluorescent intensity of each tumor tissue was quantified. $^{*}p < 0.05$ (*t*-test). Error bars indicate the mean ± S.E.

various ligands, we calculated the kinetic parameters of particular interactions. SPR analysis showed that all ligands bound to EphA10 with a high affinity (KD value of the interaction between EphA10 and EphrinA3; 1.4 nM, EphA10 and EphrinA4; 3.8 nM, EphA10 and EphrinA5; 0.89 nM) (Table 3). Their affinities (EphrinA5 ≧ EphrinA3 > EphrinA4) tend to be correlated with the rate of BrdU incorporation. These findings suggest that variation in EphA10 signaling activity and associated cellular responses is due to the affinity of particular ligands against EphA10.

3.5. Anti-EphA10 mAb accumulated in EphA10-expressing tumor tissues in vivo

In order to evaluate the behavior of anti-EphA10 mAb *in vivo*, we assessed its biodistribution in xenograft mice bearing EphA10-expressing tumors. Alexa Fluor 647-labeled anti-EphA10 mAb or control mAb was intravenously injected into the mice, with fluorescence assessed on a daily basis thereafter. *In vivo* images showed that fluorescence was non-specifically detected across the whole body of mice treated with either the anti-EphA10 mAb or the control mAb at day 2. At day 4, fluorescence accumulated more in the tumor tissues of anti-EphA10 mAb-treated mice compared to the control mAb-treated mice (Fig. 2 (A)–(X)). The ratio of fluorescent intensity of tumor tissues against that seen in the contralateral site was practically unchanged in the control antibody-treated group, while the ratio was increased within the anti-EphA10 mAb-treated group at the same timepoint (Fig. 2 (AK)). Indeed, the mean fluorescent intensity of tumor tissues isolated from dissected mice at day 4 was significantly stronger within the anti-EphA10 mAb-treated group than in the control mAb-treated group (Fig. 2 (Y)–(AJ) and (AL)). In order to validate the specificity of anti-EphA10 mAb *in vivo*, we compared the accumulation of anti-EphA10 mAb in MDA-MB-435 or MDA-MB-435^{EphA10} xenograft model mice. As a result, the mAb significantly accumulated in MDA-MB-435^{EphA10} tumor tissues compared to MDA-MB-435

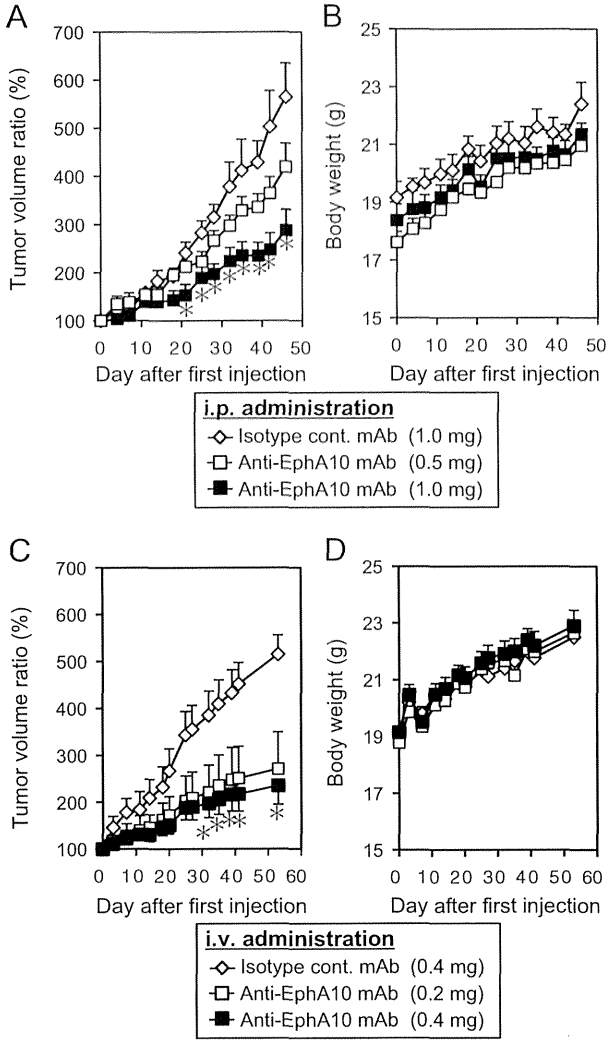

Fig. 3. *In vivo* anti-tumor effects of anti-EphA10 mAb in a xenograft mouse model. A xenograft mouse model was generated by orthotopic transplantation of MDA-MB-435 ^{EphA10} cells. When tumors reached approximately 100 mm^3 in size, (A) (B) an isotype control mAb (1.0 mg/mouse) (◇) and anti-EphA10 mAb (0.5 (□) or 1.0 (■) mg/mouse) were intraperitoneally administered twice a week. (C) (D) An isotype control mAb (0.4 mg/mouse) (◇) and anti-EphA10 mAb (0.2 (□) or 0.4 (■) mg/mouse) were intravenously administered once a week. (A) (C) Tumor volumes were measured over time and their growth ratio against the tumor volume at day 0 was compared with the control mAb group (*$p < 0.05$, one-way ANOVA). (B) (D) Body weight change in mice treated with the control mAb or anti-EphA10 mAb. Error bars indicate the mean + S.E. ($n = 5–6$).

tumor tissues (Fig. S7). Therefore, the anti-EphA10 mAb accumulated in EphA10-expressing tumor tissues, indicating its potential as an anti-tumor therapeutic tool.

3.6. Anti-EphA10 mAb caused tumor growth suppression in vivo

In order to evaluate the biological effects of the anti-EphA10 mAb accumulated in tumor tissues, we intraperitoneally administered saline, the anti-EphA10 mAb or the control mAb (1 mg/mouse) twice a week into the same xenograft mouse model. Tumor volumes increased in the saline- and the control mAb-treated groups. On the other hand, tumor growth was significantly suppressed within the anti-EphA10 mAb treated group as compared to the other groups (Fig. S8 (A)). Next, we administered the anti-EphA10 mAb (1 mg or 0.5 mg/mouse) or the control mAb (1 mg/mouse). On the basis of volume measurements, tumor growth was significantly suppressed in the case of the anti-EphA10 mAb-treated mice, with this effect occurring in a dose-dependent manner (Fig. 3 (A)). We obtained tumor tissues from dissected mice at day 47 and measured the corresponding weights. In agreement with volumetric analysis over time, tumor tissue weights were less for the anti-EphA10 mAb-treated groups, with this occurring again in a dose-dependent manner (Fig. S8 (B)). As the body weight of the mice within the different groups was unchanged during the administration (Fig. 3 (B)), indirect effects of mAb administration on body weight loss were ruled out. Furthermore, we observed anti-tumor effects *via* the same administration route (intravenous injection) as used for the biodistribution studies, in a similar vein to that obtained *via* intraperitoneal injection (Fig. 3 (C)–(D) and Fig. S8 (C)). Consequently, the mAb accumulated in EphA10-expressing tumors and significantly suppressed growth without any obvious adverse effects. These findings suggest that EphA10 is a promising drug target potentially useful for breast cancers including TNBC.

4. Discussion

EphA10, the most recent addition to the Eph family, is a relatively uncharacterized protein. Thus, its potential as a molecular target has been somewhat unclear. In this manuscript, we showed that EphA10 was specifically expressed in all subtypes of breast tumor tissues, including TNBC, but is absent in normal tissues apart from testis. The proportion of breast tumors expressing EphA10 is around 60% across all subtypes. Therefore, EphA10 expression is independent of ER, PR and Her2 status, suggesting that EphA10 targeted therapy could be utilized as a monotherapy for TNBC cases or as a combination therapy with anti-hormone and anti-Her2 drugs for luminal A, luminal B and Her2-enriched cases, as relevant. Furthermore, a key clinical problem with anti-hormone and anti-Her2 treatments is frequently tolerance to therapy over time [33–36]. Therefore, EphA10 targeted therapy may also be potentially useful in such resistant cases.

We next found that EphA10 signaling promoted DNA synthesis, which was dependent on stimulation by EphA10 ligands. However, clarification of the mechanism involved is needed. In order to elucidate the mechanistic basis underlying the interaction between EphA10 and its corresponding ligands, we examined the expression of particular ligands in tumor tissues in the context of proximity to EphA10. For this, breast cancer tissue derived from the same patient was immunostained with the mAbs against EphrinA3, A4 or A5. IHC staining revealed that all of the ligand molecules were expressed by the breast cancer cells in a similar fashion to that observed with EphA10 (Fig. S9 (A)). Moreover, their ligands were also expressed in MDA-MB-435^{EphA10} cells (Fig. S9 (B)). Therefore, one possibility is that EphA10 may be activated *via* its ligands by direct tumor cell-tumor cell contacts in breast cancer patients or MDA-MB-435^{EphA10} xenograft model mice. In future studies, it will be of interest to investigate whether anti-EphA10 can suppress signal transduction by intact Ephrins which exist on the cell membrane, as opposed to free form.

Finally, we developed a novel anti-EphA10 mAb as a therapeutic tool, showing it to accumulate in EphA10-positive tumor tissues and capable of mediating significant tumor growth suppression both *in vitro* and *in vivo*. As mentioned previously, the target protein for antibody-based drugs commonly needs to be specifically expressed in cancer tissues, so as not to cause severe adverse events in off-target tissues. We confirmed that while the anti-EphA10 mAb is also able to cross-react with mouse EphA10 (Fig. S4 (D)), the mAb tended to be restricted to tumor compared to normal tissues (Fig. 2). These data are consistent with the pattern of EphA10 protein expression observed in normal human organs (Table 2), further suggesting that the anti-EphA10 mAb could have potential as a safe drug.

Moreover, the mechanism by which the anti-EphA10 mAb inhibits ligand stimulated-proliferation is also interesting. Fig. S4 (E) showed that mAb recognized the fibronectin III (FNIII) domain within the extracellular region of EphA10, an area which consists of the ligand binding (LB) domain and the FNIII domain [6]. It has been suggested that the

FNIII domain plays an important role in the dimerization and activation of receptors [37–39]. Therefore, the inhibitory effects on proliferation may be due to reduced receptor dimerization, as opposed to competitive inhibition in respect to ligand binding. Recently, pertuzumab, a new class of anti-Her2 mAb, has demonstrated powerful and extensive anti-tumor effects in breast cancer patients by inhibiting not only homo-dimerization but also hetero-dimerization such as Her2–Her3 interactions [40,41]. It is also reported that certain Eph family members, such as EphA2 and EphB6, dimerize with other receptors, activate cancer cells and promote malignancy [10,42]. Taken together, our first-in-class anti-EphA10 mAb might have the same potency. On the other hand, it is known that Eph receptor/Ephrin signaling is associated with cancer metastasis [18–20]. We also reported that expression of EphA10 is related to lymph node metastasis in breast cancer patients [43]. It may, thus, be of interest in future work to elucidate the role of EphA10 in tumor metastasis, as well as possible therapeutic targeting of same *via* anti-EphA10 mAb.

5. Conclusions

EphA10 was specifically expressed in various subtypes of breast cancer tissues, but not within most normal tissues. Moreover, EphA10 promoted cell proliferation following ligand stimulation. Conversely, an in-house developed anti-EphA10 mAb inhibited tumor proliferation significantly at both *in vitro* and *in vivo* levels. These data should contribute to the development of novel drugs against refractory breast cancers, including TNBC.

Acknowledgments

This study was supported in part by Grants-in-Aid for Scientific Research from the Project for Development of Innovative Research on Cancer Therapeutics and the Scientific Research (C) (#26430180), the Ministry of Education, Culture, Sports, Science and Technology of Japan, and from the Japan Society for the Promotion of Science. This study was also supported in part by Health Labor Sciences Research Grants from the Ministry of Health, Labor and Welfare of Japan.

Appendix A. Supplementary data

Supplementary data to this article can be found online at http://dx.doi.org/10.1016/j.jconrel.2014.06.010.

References

[1] S.X. Lin, J. Chen, M. Mazumdar, D. Poirier, C. Wang, A. Azzi, M. Zhou, Molecular therapy of breast cancer: progress and future directions, Nat. Rev. Endocrinol. 6 (2010) 485–493.
[2] A. Ocana, J.J. Cruz, A. Pandiella, Trastuzumab and antiestrogen therapy: focus on mechanisms of action and resistance, Am. J. Clin. Oncol. 29 (2006) 90–95.
[3] L. Carey, E. Winer, G. Viale, D. Cameron, L. Gianni, Triple-negative breast cancer: disease entity or title of convenience? Nat. Rev. Clin. Oncol. 7 (2010) 683–692.
[4] S.K. Pal, B.H. Childs, M. Pegram, Triple negative breast cancer: unmet medical needs, Breast Cancer Res. Treat. 125 (2011) 627–636.
[5] F. Podo, L.M. Buydens, H. Degani, R. Hilhorst, E. Klipp, I.S. Gribbestad, S. Van Huffel, H. W. van Laarhoven, J. Luts, D. Monleon, G.J. Postma, N. Schneiderhan-Marra, F. Santoro, H. Wouters, H.G. Russnes, T. Sorlie, E. Tagliabue, A.L. Borresen-Dale, Triple-negative breast cancer: present challenges and new perspectives, Mol. Oncol. 4 (2010) 209–229.
[6] E.B. Pasquale, Eph receptor signalling casts a wide net on cell behaviour, Nat. Rev. Mol. Cell Biol. 6 (2005) 462–475.
[7] E.B. Pasquale, Eph receptors and ephrins in cancer: bidirectional signalling and beyond, Nat. Rev. Cancer 10 (2010) 165–180.
[8] J.G. Albeck, J.S. Brugge, Uncovering a tumor suppressor for triple-negative breast cancers, Cell 144 (2011) 638–640.
[9] T. Sun, N. Aceto, K.L. Meerbrey, J.D. Kessler, C. Zhou, I. Migliaccio, D.X. Nguyen, N.N. Pavlova, M. Botero, J. Huang, R.J. Bernardi, E. Schmitt, G. Hu, M.Z. Li, N. Dephoure, S.P. Gygi, M. Rao, C.J. Creighton, S.G. Hilsenbeck, C.A. Shaw, D. Muzny, R.A. Gibbs, D.A. Wheeler, C.K. Osborne, R. Schiff, M. Bentires-Alj, S.J. Elledge, T.F. Westbrook, Activation of multiple proto-oncogenic tyrosine kinases in breast cancer via loss of the PTPN12 phosphatase, Cell 144 (2011) 703–718.
[10] D.M. Brantley-Sieders, G. Zhuang, D. Hicks, W.B. Fang, Y. Hwang, J.M. Cates, K. Coffman, D. Jackson, E. Bruckheimer, R.S. Muraoka-Cook, J. Chen, The receptor tyrosine kinase EphA2 promotes mammary adenocarcinoma tumorigenesis and metastatic progression in mice by amplifying ErbB2 signaling, J. Clin. Invest. 118 (2008) 64–78.
[11] N. Munarini, R. Jager, S. Abderhalden, G. Zuercher, V. Rohrbach, S. Loercher, B. Pfanner-Meyer, A.C. Andres, A. Ziemiecki, Altered mammary epithelial development, pattern formation and involution in transgenic mice expressing the EphB4 receptor tyrosine kinase, J. Cell Sci. 115 (2002) 25–37.
[12] D.P. Zelinski, N.D. Zantek, J.C. Stewart, A.R. Irizarry, M.S. Kinch, EphA2 overexpression causes tumorigenesis of mammary epithelial cells, Cancer Res. 61 (2001) 2301–2306.
[13] S.R. Kumar, J. Singh, G. Xia, V. Krasnoperov, L. Hassanieh, E.J. Ley, J. Scehnet, N.G. Kumar, D. Hawes, M.F. Press, F.A. Weaver, P.S. Gill, Receptor tyrosine kinase EphB4 is a survival factor in breast cancer, Am. J. Pathol. 169 (2006) 279–293.
[14] K.A. Mohammed, X. Wang, E.P. Goldberg, V.B. Antony, N. Nasreen, Silencing receptor EphA2 induces apoptosis and attenuates tumor growth in malignant mesothelioma, Am. J. Cancer Res. 1 (2011) 419–431.
[15] N.K. Noren, M. Lu, A.L. Freeman, M. Koolpe, E.B. Pasquale, Interplay between EphB4 on tumor cells and vascular ephrin-B2 regulates tumor growth, Proc. Natl. Acad. Sci. U. S. A. 101 (2004) 5583–5588.
[16] S. Sawamiphak, S. Seidel, C.L. Essmann, G.A. Wilkinson, M.E. Pitulescu, T. Acker, A. Acker-Palmer, Ephrin-B2 regulates VEGFR2 function in developmental and tumour angiogenesis, Nature 465 (2010) 487–491.
[17] Y. Wang, M. Nakayama, M.E. Pitulescu, T.S. Schmidt, M.L. Bochenek, A. Sakakibara, S. Adams, A. Davy, U. Deutsch, U. Luthi, A. Barberis, L.E. Benjamin, T. Makinen, C.D. Nobes, R.H. Adams, Ephrin-B2 controls VEGF-induced angiogenesis and lymphangiogenesis, Nature 465 (2010) 483–486.
[18] D.M. Brantley-Sieders, W.B. Fang, D.J. Hicks, G. Zhuang, Y. Shyr, J. Chen, Impaired tumor microenvironment in EphA2-deficient mice inhibits tumor angiogenesis and metastatic progression, FASEB J. 19 (2005) 1884–1886.
[19] M.S. Duxbury, H. Ito, M.J. Zinner, S.W. Ashley, E.E. Whang, EphA2: a determinant of malignant cellular behavior and a potential therapeutic target in pancreatic adenocarcinoma, Oncogene 23 (2004) 1448–1456.
[20] X.D. Ji, G. Li, Y.X. Feng, J.S. Zhao, J.J. Li, Z.J. Sun, S. Shi, Y.Z. Deng, J.F. Xu, Y.Q. Zhu, H.P. Koeffler, X.J. Tong, D. Xie, EphB3 is overexpressed in non-small-cell lung cancer and promotes tumor metastasis by enhancing cell survival and migration, Cancer Res. 71 (2011) 1156–1166.
[21] D. Jackson, J. Gooya, S. Mao, K. Kinneer, L. Xu, M. Camara, C. Fazenbaker, R. Fleming, S. Swamynathan, D. Meyer, P.D. Senter, C. Gao, H. Wu, M. Kinch, S. Coats, P.A. Kiener, D.A. Tice, A human antibody-drug conjugate targeting EphA2 inhibits tumor growth in vivo, Cancer Res. 68 (2008) 9367–9374.
[22] J.W. Lee, H.D. Han, M.M. Shahzad, S.W. Kim, L.S. Mangala, A.M. Nick, C. Lu, R.R. Langley, R. Schmandt, H.S. Kim, S. Mao, J. Gooya, C. Fazenbaker, D. Jackson, D.A. Tice, C.N. Landen, R.L. Coleman, A.K. Sood, EphA2 immunoconjugate as molecularly targeted chemotherapy for ovarian carcinoma, J. Natl. Cancer Inst. 101 (2009) 1193–1205.
[23] J.W. Lee, R.L. Stone, S.J. Lee, E.J. Nam, J.W. Roh, A.M. Nick, H.D. Han, M.M. Shahzad, H. S. Kim, L.S. Mangala, N.B. Jennings, S. Mao, J. Gooya, D. Jackson, R.L. Coleman, A.K. Sood, EphA2 targeted chemotherapy using an antibody drug conjugate in endometrial carcinoma, Clin. Cancer Res. 16 (2010) 2562–2570.
[24] C.M. Annunziata, E.C. Kohn, P. LoRusso, N.D. Houston, R.L. Coleman, M. Buzoianu, G. Robbie, R. Lechleider, Phase 1, open-label study of MEDI-547 in patients with relapsed or refractory solid tumors, Invest. New Drugs 31 (2013) 77–84.
[25] S. Imai, K. Nagano, Y. Yoshida, T. Okamura, T. Yamashita, Y. Abe, T. Yoshikawa, Y. Yoshioka, H. Kamada, Y. Mukai, S. Nakagawa, Y. Tsutsumi, S. Tsunoda, Development of an antibody proteomics system using a phage antibody library for efficient screening of biomarker proteins, Biomaterials 32 (2011) 162–169.
[26] H.C. Aasheim, S. Patzke, H.S. Hjorthaug, E.F. Finne, Characterization of a novel Eph receptor tyrosine kinase, EphA10, expressed in testis, Biochim. Biophys. Acta 1723 (2005) 1–7.
[27] K.E. Huber, L.A. Carey, D.E. Wazer, Breast cancer molecular subtypes in patients with locally advanced disease: impact on prognosis, patterns of recurrence, and response to therapy, Semin. Radiat. Oncol. 19 (2009) 204–210.
[28] P.J. Roberts, C.J. Der, Targeting the Raf-MEK-ERK mitogen-activated protein kinase cascade for the treatment of cancer, Oncogene 26 (2007) 3291–3310.
[29] I. Zachary, VEGF signalling: integration and multi-tasking in endothelial cell biology, Biochem. Soc. Trans. 31 (2003) 1171–1177.
[30] H. Zhong, J.P. Bowen, Molecular design and clinical development of VEGFR kinase inhibitors, Curr. Top. Med. Chem. 7 (2007) 1379–1393.
[31] B. Boilly, A.S. Vercoutter-Edouart, H. Hondermarck, V. Nurcombe, X. Le Bourhis, FGF signals for cell proliferation and migration through different pathways, Cytokine Growth Factor Rev. 11 (2000) 295–302.
[32] M.B. Buck, C. Knabbe, TGF-beta signaling in breast cancer, Ann. N. Y. Acad. Sci. 1089 (2006) 119–126.
[33] H.J. Johansson, B.C. Sanchez, F. Mundt, J. Forshed, A. Kovacs, E. Panizza, L. Hultin-Rosenberg, B. Lundgren, U. Martens, G. Mathe, Z. Yakhini, K. Helou, K. Krawiec, L. Kanter, A. Hjerpe, O. Stal, B.K. Linderholm, J. Lehtio, Retinoic acid receptor alpha is associated with tamoxifen resistance in breast cancer, Nat. Commun. 4 (2013) 2175.
[34] M. Scaltriti, P.J. Eichhorn, J. Cortes, L. Prudkin, C. Aura, J. Jimenez, S. Chandarlapaty, V. Serra, A. Prat, Y.H. Ibrahim, M. Guzman, M. Gili, O. Rodriguez, S. Rodriguez, J. Perez, S. R. Green, S. Mai, N. Rosen, C. Hudis, J. Baselga, Cyclin E amplification/overexpression is a mechanism of trastuzumab resistance in HER2+ breast cancer patients, Proc. Natl. Acad. Sci. U. S. A. 108 (2011) 3761–3766.
[35] S.L. Tilghman, I. Townley, Q. Zhong, P.P. Carriere, J. Zou, S.D. Llopis, L.C. Preyan, C.C. Williams, E. Skripnikova, M.R. Bratton, Q. Zhang, G. Wang, Proteomic signatures of acquired letrozole resistance in breast cancer: suppressed estrogen signaling and increased cell motility and invasiveness, Mol. Cell. Proteomics 12 (2013) 2440–2455.

[36] S. Zhang, W.C. Huang, P. Li, H. Guo, S.B. Poh, S.W. Brady, Y. Xiong, L.M. Tseng, S.H. Li, Z. Ding, A.A. Sahin, F.J. Esteva, G.N. Hortobagyi, D. Yu, Combating trastuzumab resistance by targeting SRC, a common node downstream of multiple resistance pathways, Nat. Med. 17 (2011) 461–469.
[37] J.O. Moore, M.A. Lemmon, K.M. Ferguson, Tie2 receptor dimerization mediated by its extracellular FNIII domains, Biophysical Journal, 2013, p. 608a.
[38] M.A. Schumacher, N. Chinnam, T. Ohashi, R.S. Shah, H. Erickson, Structure of irisin reveals a novel intersubunit beta-sheet fibronectin (FNIII) dimer; implications for receptor activation, J. Biol. Chem. 288 (2013) 33738–33744.
[39] L. Zabeau, D. Defeau, H. Iserentant, J. Vandekerckhove, F. Peelman, J. Tavernier, Leptin receptor activation depends on critical cysteine residues in its fibronectin type III subdomains, J. Biol. Chem. 280 (2005) 22632–22640.
[40] G.M. Keating, Pertuzumab: in the first-line treatment of HER2-positive metastatic breast cancer, Drugs 72 (2012) 353–360.
[41] S.M. Swain, S.B. Kim, J. Cortes, J. Ro, V. Semiglazov, M. Campone, E. Ciruelos, J.M. Ferrero, A. Schneeweiss, A. Knott, E. Clark, G. Ross, M.C. Benyunes, J. Baselga, Pertuzumab, trastuzumab, and docetaxel for HER2-positive metastatic breast cancer (CLEOPATRA study): overall survival results from a randomised, double-blind, placebo-controlled, phase 3 study, Lancet Oncol. 14 (2013) 461–471.
[42] A. Freywald, N. Sharfe, C.M. Roifman, The kinase-null EphB6 receptor undergoes transphosphorylation in a complex with EphB1, J. Biol. Chem. 277 (2002) 3823–3828.
[43] K. Nagano, S. Kanasaki, T. Yamashita, Y. Maeda, M. Inoue, K. Higashisaka, Y. Yoshioka, Y. Abe, Y. Mukai, H. Kamada, Y. Tsutsumi, S. Tsunoda, Expression of Eph receptor A10 is correlated with lymph node metastasis and stage progression in breast cancer patients, Cancer Med. 2 (2013) 972–977.

Regular Article

THROMBOSIS AND HEMOSTASIS

Anti-factor IXa/X bispecific antibody ACE910 prevents joint bleeds in a long-term primate model of acquired hemophilia A

Atsushi Muto,[1] Kazutaka Yoshihashi,[1] Minako Takeda,[1] Takehisa Kitazawa,[1] Tetsuhiro Soeda,[1] Tomoyuki Igawa,[1] Zenjiro Sampei,[1] Taichi Kuramochi,[1] Akihisa Sakamoto,[1] Kenta Haraya,[1] Kenji Adachi,[1] Yoshiki Kawabe,[1] Keiji Nogami,[2] Midori Shima,[2] and Kunihiro Hattori[1]

[1]Research Division, Chugai Pharmaceutical Co, Ltd, Gotemba, Shizuoka, Japan; and [2]Department of Pediatrics, Nara Medical University, Kashihara, Nara, Japan

Key Points

- A long-term acquired hemophilia A model expressing spontaneous joint bleeds and other bleeds was newly established in nonhuman primates.
- Weekly SC dose of the anti-FIXa/X bispecific antibody ACE910 prevented joint bleeds and other bleeds in the primate hemophilia A model.

ACE910 is a humanized anti-factor IXa/X bispecific antibody mimicking the function of factor VIII (FVIII). We previously demonstrated in nonhuman primates that a single IV dose of ACE910 exerted hemostatic activity against hemophilic bleeds artificially induced in muscles and subcutis, and that a subcutaneous (SC) dose of ACE910 showed a 3-week half-life and nearly 100% bioavailability, offering support for effective prophylaxis for hemophilia A by user-friendly SC dosing. However, there was no direct evidence that such SC dosing of ACE910 would prevent spontaneous bleeds occurring in daily life. In this study, we newly established a long-term primate model of acquired hemophilia A by multiple IV injections of an anti-primate FVIII neutralizing antibody engineered in mouse-monkey chimeric form to reduce its antigenicity. The monkeys in the control group exhibited various spontaneous bleeding symptoms as well as continuous prolongation of activated partial thromboplastin time; notably, all exhibited joint bleeds, which are a hallmark of hemophilia. Weekly SC doses of ACE910 (initial 3.97 mg/kg followed by 1 mg/kg) significantly prevented these bleeding symptoms; notably, no joint bleeding symptoms were observed. ACE910 is expected to prevent spontaneous bleeds and joint damage in hemophilia A patients even with weekly SC dosing, although appropriate clinical investigation is required. (*Blood.* 2014;124(20): 3165-3171)

Introduction

Patients with severe hemophilia A (<1% of normal factor VIII [FVIII] level) typically suffer from recurrent bleeding episodes, primarily in the musculoskeletal system.[1,2] Approximately 85% of the bleeding episodes are into joints,[3] and repeated joint bleeding from early childhood results in a chronic degenerative arthritis. Although traditional on-demand treatment by a FVIII agent cannot prevent hemophilic arthropathy, routine prophylaxis with FVIII to maintain ≥1% FVIII:C is beneficial in preventing it.[4,5] However, the need for frequent IV injections of FVIII negatively affects patients' quality of life and their adherence to the routine prophylactic regimen, which is particularly problematic when treating pediatric patients at home.[2,6]

Furthermore, ~30% of severe patients develop alloantibodies against FVIII (FVIII inhibitors),[2,7] which largely restrict treatment with FVIII. FVIII inhibitors make hemorrhage more difficult to be controlled because alternative bypassing agents have shorter half-lives and are not always effective.[7,8] Attempts to induce immune tolerance to FVIII inhibitors with high doses of FVIII are very expensive and do not always work.[9]

Therefore, a novel drug is needed: one that is long-lasting, subcutaneously injectable, effective regardless of FVIII inhibitors, and does not induce FVIII inhibitors.[10-13] To achieve this desirable profile, we produced a series of humanized immunoglobulin G (IgG) antibodies bispecific to factors IXa and X (anti-FIXa/X antibodies) that mimic the FVIII cofactor function by binding and placing FIXa and FX into spatially appropriate positions (supplemental Figure 1, see supplemental Data available on the *Blood* Web site),[14] and identified a clinical investigational drug termed ACE910.[15] In a short-term primate model of acquired hemophilia A, ACE910 at a single IV dose of 1 or 3 mg/kg exerted hemostatic activity against artificial ongoing bleeds in muscles and subcutis to the same extent as recombinant porcine FVIII (rpoFVIII) at twice-daily IV doses of 10 U/kg.[16] Furthermore, a multiple-dosing simulation calculated from the pharmacokinetic (PK) parameters of ACE910 in cynomolgus monkeys suggested that the plasma ACE910 concentration capable of stopping even ongoing bleeds would be maintained by once-weekly subcutaneous (SC) administration of 0.64 to 1.5 mg/kg ACE910.[16]

Submitted July 2, 2014; accepted September 14, 2014. Prepublished online as *Blood* First Edition paper, October 1, 2014; DOI 10.1182/blood-2014-07-585737.

Presented in abstract form at the World Federation of Hemophilia 2014 World Congress, Melbourne, Australia, May 11-15, 2014.

The online version of this article contains a data supplement.

The publication costs of this article were defrayed in part by page charge payment. Therefore, and solely to indicate this fact, this article is hereby marked "advertisement" in accordance with 18 USC section 1734.

Prevention of joint bleeding is of major importance in the care of hemophilia A patients.[3] However, it remained unproven whether repeated SC dosing of ACE910 could actually prevent spontaneous bleeding episodes, including the joint bleeds that are a pathologic hallmark of hemophilia A. To address this question nonclinically, we required a primate model because ACE910 is highly species-specific in its FVIII-mimetic cofactor activity.[16]

In this study, we aimed first to establish a long-term acquired hemophilia A model expressing spontaneous bleeding episodes, including joint bleeds, in nonhuman primates, and second to evaluate the preventive effect of once-weekly SC dosing of ACE910 in this model for investigating the potential of a prophylactic treatment in hemophilia A patients.

Materials and methods

ACE910

ACE910 was expressed in HEK293 or CHO cells cotransfected with a mixture of plasmids encoding the anti-FIXa heavy chain, anti-FX heavy chain, and common light chain.[15] ACE910 was purified by protein A and ion-exchange chromatography from the culture supernatants.

Anti-primate FVIII neutralizing antibodies

A mouse monoclonal anti-primate FVIII neutralizing antibody, termed VIII-2236, was prepared from hybridoma culture supernatants.[14,16] A chimeric mouse-monkey anti-primate FVIII neutralizing antibody, termed cyVIII-2236, was constructed comprising the mouse variable region from VIII-2236 and the monkey constant region of IgG, which we originally cloned from cynomolgus monkey thymus. The cyVIII-2236 antibody was produced in HEK293 cells and isolated by protein A and gel permeation chromatography from the culture supernatants.

Comparison of cyVIII-2236 with VIII-2236 in an APTT assay

First, to compare the FVIII-neutralizing activity between cyVIII-2236 and VIII-2236, each was added to citrated plasma pooled from 3 normal male cynomolgus monkeys. Then, activated partial thromboplastin time (APTT) was measured with a standard method using Thrombocheck APTT-SLA (Sysmex) and coagulation analyzer KC4 Delta (Stago). Second, to compare the effect of cyVIII-2236 and VIII-2236 on the APTT-shortening activity of ACE910, each was added to FVIII-deficient human plasma (George King) at the final plasma concentration of 300 μg/mL together with various concentrations of ACE910, then APTT was measured.

Animals

Ten male cynomolgus monkeys (2.35-4.25 kg, aged 3-4 years) were purchased from Hamri. All animal studies were approved by the institutional animal care and use committee of Chugai Pharmaceutical, and were conducted in accordance with the approved protocols and the Guidelines for the Care and Use of Laboratory Animals at the company. Chugai Pharmaceutical is fully accredited by the Association for Assessment and Accreditation of Laboratory Animal Care (AAALAC) International.

Long-term primate model of acquired hemophilia A

In the first part of this study, 2 cynomolgus monkeys received weekly IV injections (3 or 10 mg/kg each) of VIII-2236. Citrated blood was collected over time. Blood hemoglobin (Hgb) concentration was measured by hematology analyzer SF-3000 (Sysmex) to monitor hemorrhagic anemia. APTT was assessed with a standard method using Data-Fi APTT (Siemens) and coagulation analyzer AMAX CS-190 (Trinity). In addition, bleeding symptoms (bruises [dark-red areas on the body surface], hematuria, limping, and general condition including joint swelling) were monitored on 21 working days from day 0 until day 28. To observe bruises easily, the body hair was sheared on day 0, and the area of bruises and the number of days when bruises had been detected were assessed.

In the second part of this study, another 8 cynomolgus monkeys received weekly IV injections (10 mg/kg) of cyVIII-2236. Two groups (n = 4 each) were established: a control group (the vehicle group) treated with vehicle and a test group (the ACE910 group) treated with ACE910. ACE910 was administered as an initial 3.97 mg/kg SC dose 2 hours after cyVIII-2236 injection on day 0, and thereafter as weekly 1 mg/kg SC doses. The same dosing regimen of vehicle (histidine buffer containing a surfactant) was applied to the vehicle group. Citrated blood was collected over time. Blood Hgb concentration was measured; the change in blood Hgb level was expressed as a percentage of that on day 0 (2 hours after cyVIII-2236 injection). APTT was measured with Thrombocheck APTT-SLA and KC4 Delta. Bleeding symptoms were monitored on 41 working days until day 56. Necropsy was performed on day 56; organs and tissues from the whole body were macroscopically examined, and hemorrhagic findings in joints (shoulder, elbow, wrist, hip, knee, and ankle on both sides) were scored. Then, they were histopathologically examined.

We assessed cyVIII-2236 concentration, FVIII-neutralizing titer of cyVIII-2236, ACE910 concentration, and development of anti-ACE910 alloantibodies. The methods are described in detail in the supplemental Methods. Briefly, cyVIII-2236 concentration was determined with a sandwich enzyme-linked immunosorbent assay (ELISA) using recombinant human FVIII and an anti-human IgG antibody. FVIII-neutralizing titers of cyVIII-2236 on days 0 (just after cyVIII-2236 injection) and 56 were assessed with a modified Bethesda assay. ACE910 concentration was determined with a sandwich ELISA to quantify human IgG.[16] Anti-ACE910 alloantibodies present at necropsy were examined with an electrochemiluminescent bridging immunoassay using labeled ACE910.[16]

In both parts, the monkeys were carefully monitored under the supervision of the attending veterinarian to determine the necessity of pain relief or other treatment. Consequently, no monkeys received an analgesic drug.

Statistical analysis and multiple-dosing simulation

The data are presented as individual values or as mean ± standard deviation (SD). In the in vivo efficacy study, some were analyzed by 2-tailed Student *t* test (SAS Preclinical Package, version 5.00) between the vehicle and the ACE910 groups. A *P* value of .05 or less was considered statistically significant. Multiple doses of ACE910 were simulated on the basis of the PK parameters previously determined[16] with SAAM II, version 1.2 software (SAAM Institute).

Results

Failure of long-term neutralization of endogenous FVIII by VIII-2236 in cynomolgus monkeys

First, we attempted to establish a long-term acquired hemophilia A model by weekly IV injection of VIII-2236 in cynomolgus monkeys. APTT prolongation was observed for the first 2 weeks (Figure 1), but gradually shortened after the third injection, and finally disappeared by the end of the fourth week, suggesting the development of alloantibodies to VIII-2236. VIII-2236 is a mouse IgG, and therefore entirely foreign to primates. In addition, no sign of joint bleeds was observed, although some bruises and a transient decrease in blood Hgb were detected (data not shown). Consequently, we sought an alternative way of establishing a longer-term primate model of acquired hemophilia A.

Chimerization of VIII-2236 to cyVIII-2236

As an attempt to avoid anti-VIII-2236 alloantibody development, we chimerized VIII-2236 (mouse IgG) by replacing its constant region with that of cynomolgus monkey IgG. The chimerized VIII-2236

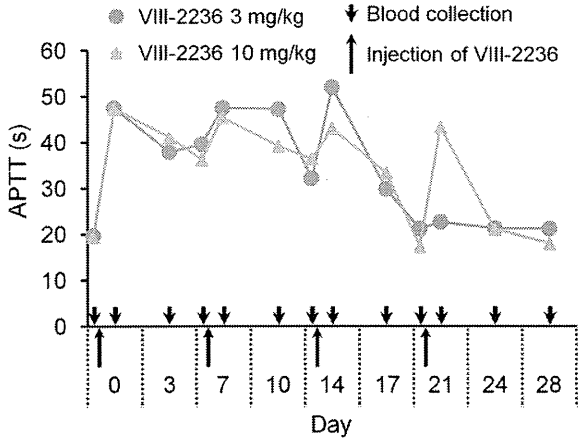

Figure 1. Change in APTT after weekly IV injection of the mouse anti-primate FVIII neutralizing antibody VIII-2236 in cynomolgus monkeys. VIII-2236 was injected at 3 or 10 mg/kg IV doses to cynomolgus monkeys on days 0, 7, 14, and 21. Citrated blood was collected on days 0, 3, 7, 10, 14, 17, 21, 24, and 28 (before and 2 hours after VIII-2236 injection on days 0, 7, 14, and 21). The time course of APTT is shown for each monkey.

(cyVIII-2236) successfully prolonged APTT in cynomolgus monkey plasma in vitro with a similar concentration dependency to that of original VIII-2236 (Figure 2A). Additionally, cyVIII-2236 did not interfere with the APTT-shortening activity of ACE910, the same results were also found with VIII-2236 (Figure 2B). These results indicate that VIII-2236 was successfully chimerized to cyVIII-2236 while retaining the original characteristics.

Establishment of a long-term acquired hemophilia A model expressing spontaneous joint bleeds in cynomolgus monkeys

Using cyVIII-2236, we retried to establish long-term neutralization of endogenous FVIII, expecting reproducible development of spontaneous joint bleeds. The experimental protocol is illustrated in Figure 3A. In all the monkeys given vehicle (n = 4), APTT was prolonged to approximately twice the normal baseline for 8 weeks (Figure 3B). Plasma cyVIII-2236 concentration fluctuated, but remained over 58.6 μg/mL (nearly 400 nM) (supplemental Figure 2). As over 400 nM cyVIII-2236 prolonged APTT by twofold in vitro (Figure 2A), these observations seemed consistent. Thus, an acquired hemophilia A state was successfully maintained by using cyVIII-2236.

In this long-lasting acquired hemophilia A state, all the control monkeys given vehicle developed abnormal leg motion known as limping: a behavior to avoid using the affected leg (Figure 3C). The limping continued until the experiments ended, with days when limping was detected reaching 25.0 ± 8.3 days (61% ± 20%) of the 41 observation days. Two control monkeys (#3 and #4) developed joint swelling at the ankle in the limping limb from days 28 to 42 and from days 18 to 42, respectively. Macroscopic observation at necropsy on day 56 revealed intraarticular dark red areas (consistent with hemorrhagic findings in the histopathological examination) in joints (elbow, hip, or ankle) of all the control monkeys; the number of bleeding joints was 2.0 ± 0.8 per head (Figure 3D, Table 1). Bleeding was detected in the hip or ankle joint of the side that limped. Representative macroscopic findings of the hip joints are shown in Figures 3Ei-ii. Hemorrhagic findings or reactive findings associated with hemorrhage were histopathologically confirmed in the joints that limped: hemorrhage/hemosiderin deposition, mononuclear cell infiltration, and vascular proliferation in the synovial membranes; synovial hyperplasia; granulation tissue; and destruction of articular cartilage or underlying bone (Figure 4A-C). Thus, a long-term acquired hemophilia A model expressing spontaneous joint bleeds was successfully established in cynomolgus monkeys.

Other spontaneous bleeding symptoms, that is, bruises and hematuria, were detected by daily observation in the vehicle group (data not shown). By macroscopic observation at necropsy, hemorrhagic findings were also observed in skeletal muscle (lower abdomen and femoral region), urinary bladder, seminal vesicle, rectum, and subcutis (back) in 1 or 2 of the 4 control monkeys (Table 1). Additionally, blood Hgb temporarily decreased during the observation period with the lowest values reaching 64% to 87% (Figure 5), suggesting substantial hemorrhagic blood loss.

Bleeding preventive effect of ACE910 in the long-term acquired hemophilia A model

The preventive effect of a weekly SC dose of ACE910 on spontaneous joint bleeds was evaluated in the model described in "Establishment of a long-term acquired hemophilia A model expressing spontaneous joint bleeds in cynomolgus monkeys." The dosing regimen was simulated to maintain the plasma concentration trough at >30 μg/mL from the first week after administration using the PK parameters of ACE910 in cynomolgus monkeys previously obtained because around 26 μg/mL of plasma ACE910 would show hemostatic activity

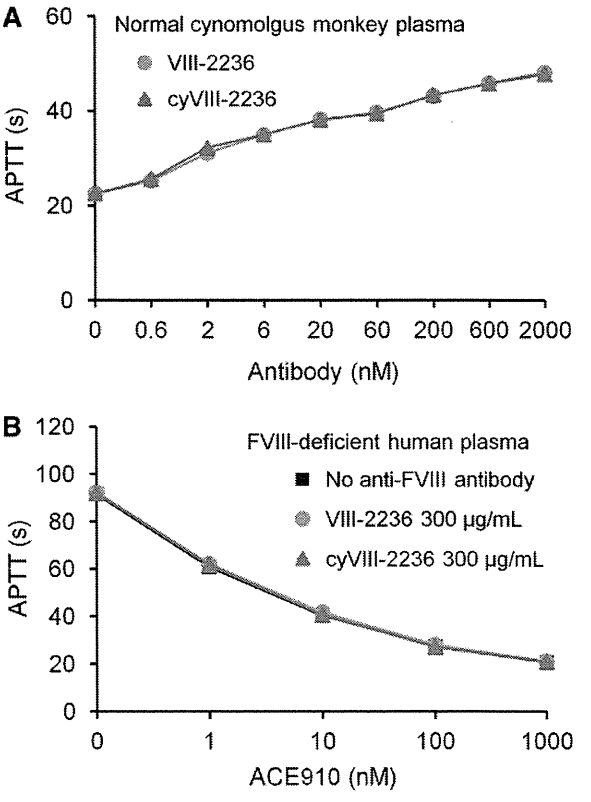

Figure 2. Comparison of the mouse-monkey chimeric anti-primate FVIII neutralizing antibody cyVIII-2236 with the original mouse antibody VIII-2236 in an APTT assay. (A) Effects of cyVIII-2236 and VIII-2236 on APTT in normal cynomolgus monkey plasma. (B) Influence of 300 μg/mL cyVIII-2236 and VIII-2236 on APTT-shortening activity of ACE910 in FVIII-deficient human plasma. Data are expressed as means ± SD (n = 3). The bars depicting SD are shorter than the height of the symbols. The symbols for the group without anti-FVIII antibody are hidden behind the symbols for the other groups in panel B.